

SEPTEMBER 2018

M.Sc. in Aircraft and Space Engineering

ÜMIT KORKMAZ

**UNIVERSITY OF GAZIANTEP
GRADUATE SCHOOL OF
NATURAL & APPLIED SCIENCES**

DESIGN OF ADJUSTABLE AIRFOIL TO DELAY STALL

M. Sc. THESIS

IN

AIRCRAFT AND AEROSPACE ENGINEERING

BY

ÜMIT KORKMAZ

SEPTEMBER 2018

Design of Adjustable Airfoil to Delay Stall

**M.Sc. Thesis
in
Aircraft and Space Engineering
University of Gaziantep**



**Supervisor
Assoc. Prof. Dr. İbrahim GÖV**

**Co-Supervisor
Assist. Prof. Dr. Mehmet Hanifi DOĞRU**

by

Ümit KORKMAZ

September 2018



© 2018 [Ümit KORKMAZ]

REPUBLIC OF TURKEY
UNIVERSITY OF GAZIANTEP
GRADUATE SCHOOL OF NATURAL & APPLIED SCIENCES
AIRCRAFT AND AEROSPACE ENGINEERING

Name of the thesis: Design of Adjustable Airfoil to Delay Stall

Name of the student: Ümit KORKMAZ


Exam date: 07.09.2018

Approval of the Graduate School of Natural and Applied Sciences

Prof. Dr. A. Necmeddin YAZICI

Director

I certify that this thesis satisfies all the requirements as a thesis for the degree of
Master of Science.


Asst. Prof. Dr. M. Orkun ÖĞÜCÜ

Head of Department

This is to certify that we have read this thesis and that in our opinion it is fully
adequate, in scope and quality, as a thesis for the degree of Master of Science.


Asst. Prof. Dr. Mehmet Hanifi DOĞRU

Co-Supervisor


Assoc. Prof. Dr. İbrahim GÖV

Supervisor

Examining Committee Members:

Assoc. Prof. Dr. İbrahim GÖV

Asst. Prof. Dr. Tahir DURHASAN

Asst. Prof. Dr. Sohayb Abdul KARIM

Signature


.....

.....

.....

I hereby declare that all information in this document has been obtained and presented in accordance with academic rules and ethical conduct. I also declare that, as required by these rules and conduct, I have fully cited and referenced all material and results that are not original to this work.

Ümit KORKMAZ

ABSTRACT

DESIGN OF ADJUSTABLE AIRFOIL TO DELAY STALL

KORKMAZ, Ümit

M.Sc. in Aircraft and Aerospace Engineering

Supervisor: Assoc. Prof. Dr. İbrahim GÖV

Co-Supervisor: Asst.Prof. Dr. M. Hanifi DOĞRU

September 2018

51 pages

In this study an alternative method is developed to reduce flow separation. Control of flow separation and transition point by means of different mechanisms such as using leading edge devices, blowing, and suction have been quite extensively researched in the literature. In this study, a new concept is investigated: Airfoil shape can be changed dynamically at different conditions (such as speed, angle of attack) also unusual airfoil design constraints can sometimes arise leading to some unconventional shapes and as a result of these designs different airfoil models can be used when the aircraft is climbing or descending. This property contribute high efficiency at any angle of attack or speed. To prove this efficiency the existing wing models (NACA 4412 and NACA 63-215) were changed to make comparisons at different angles of attack. In this study, the aerodynamic characteristics of the new wing profiles obtained by changing the x / c ratio of the two wing types (NACA 4412 and NACA 63-215) were investigated. It has been observed that the stall condition can be delayed between about 2 and 4 degrees due to the increase in maximum lift force in the wings at the end of the operation.

Key Words: Flow Separation, Airfoil Shape Design and Different Angles of Attack

ÖZET

AKIŞ AYRILMASINI GECİKTİRMEK İÇİN AYARLANABİLİR KANAT PROFİLİ TASARLAMA

KORKMAZ, Ümit

Yüksek Lisans Tezi, Uçak ve Uzay Mühendisliği

Danışman: Doç. Dr. İbrahim GÖV

Yardımcı Danışman: Dr. Öğr. Üyesi M. Hanifi DOĞRU

Eylül 2018

51 sayfa

Bu çalışmada, akış ayrılmasını azaltmak için alternatif bir yöntem geliştirilmiştir. Literatürde akış ayrılması ve geçiş noktasının üfleme ve emiş gibi farklı mekanizmalarla kontrol edilmesi oldukça kapsamlı bir şekilde araştırılmıştır. Bu çalışmada yeni bir konsept araştırılmıştır: Kanat şekli farklı koşullarda (örneğin hız, hucüm açısı) dinamik olarak değiştirilebilmektedir ve bazen bu tasarımlarla alışılmışın dışında şekiller elde edilebilir ve bu tasarımların bir sonucu olarak, uçak tırmanırken veya inerken bu farklı tasarım kanat modelleri kullanılabilir. Bu yeni özellik herhangi bir hücum açısında veya hızda yüksek verime katkıda bulunur. Bu verimi ispatlamak için mevcut kanat modelleri (NACA 4412 ve NACA 63-215) değiştirilerek farklı hücum açıları karşılaştırmalar yapıldı. Bu çalışmada, iki kanat tipinin (NACA 4412 ve NACA 63-215) x / c oranının değiştirilerek elde edilen yeni kanat profillerinin aerodinamik özellikleri araştırılmıştır. Operasyonun sonunda stall durumunun, kanatlardaki maksimum kaldırma kuvvetindeki artıştan dolayı yaklaşık 2 ila 4 derece arasında geciktirilebildiği görülmüştür.

Anahtar Kelimeler: Akış Ayrılması, Kanat Şekli Dizayn ve Farklı Hücum Açılıarı



To my family....

ACKNOWLEDGEMENTS

I would like to express my deep gratitude to Assoc. Prof. Dr. İbrahim GÖV my research supervisor and Asst. Prof. Dr. M. Hanifi DOĞRU my research CO-supervisor for enthusiastic encouragement and useful critiques of this research work.

Finally, I wish to thank my parents, my wife and friends for their support and encouragement throughout my study.

TABLE OF CONTENTS

| | Page |
|---|-------------|
| ABSTRACT | v |
| ÖZET | vi |
| ACKNOWLEDGEMENTS | viii |
| TABLE OF CONTENTS | ix |
| LIST OF FIGURES | xi |
| LIST OF SYMBOLS | xiv |
| CHAPTER 1. INTRODUCTION | 1 |
| 1.1 General Introduction | 1 |
| 1.2 Research Objectives and Tasks | 2 |
| 1.3 Layout of Thesis..... | 3 |
| CHAPTER 2. LITERATURE REVIEW | 4 |
| 2.1 General Aerodynamics Studies | 5 |
| 2.2 Active Flow Control Studies | 7 |
| 2.3 Passive Flow Control Studies | 8 |
| CHAPTER 3. COMPUTATIONAL FLUID DYNAMIC | 10 |
| 3.1 Navier-Stokes Equations..... | 10 |
| 3.2 Finite Element Method..... | 11 |
| 3.3 ANSYS Software | 12 |
| CHAPTER 4. STALL | 15 |
| 4.1 Flow Separation | 16 |
| 4.2 Stall Warning Systems | 17 |
| CHAPTER 5. CASE STUDIES OF ADJUSTABLE AIRFOIL DESIGN | 19 |
| 5.1 Introduction | 19 |
| 5.2 Analysis..... | 20 |
| 5.3 Adjustable NACA 4412 Profile Design | 22 |
| 5.4 Adjustable NACA 63-215 Profile Design | 33 |

| | |
|---|-----------|
| CHAPTER 6. RESULTS AND DISCUSIONS..... | 44 |
| CHAPTER 7. CONCLUSION | 46 |
| CHAPTER 8. FUTURE WORKS | 48 |
| REFERENCES..... | 49 |



LIST OF FIGURES

| | Page |
|---|-------------|
| Figure 3.1 Computational fluid dynamics..... | 10 |
| Figure 3.2 Divided domain..... | 12 |
| Figure 3.3 Design domain | 13 |
| Figure 3.4 Mesh model..... | 13 |
| Figure 3.5 Setup-boundary conditions | 14 |
| Figure 3.6 Results tool box | 14 |
| Figure 4.1 Stall situation | 15 |
| Figure 4.2 Critic angle of attack & maximum lift coefficient..... | 16 |
| Figure 4.3 Flow seperation..... | 16 |
| Figure 4.4 Schematic flow seperation..... | 17 |
| Figure 4.5 Stall warning sytem | 18 |
| Figure 5.1 Lift force, drag force and angle of attack..... | 19 |
| Figure 5.2 Mesh accuarcy | 21 |
| Figure 5.3 NACA 4412 and 2 improved airfoils..... | 22 |
| Figure 5.4 Complete mesh | 23 |
| Figure 5.5 Enlarged view of NACA 4412 and improved NACA 4412 mesh..... | 23 |
| Figure 5.6 Lift coefficient at different AoA | 24 |
| Figure 5.7 Drag coefficient at different AoA | 24 |
| Figure 5.8 Cl/Cd at different AoA | 25 |
| Figure 5.9 Pressure distribution of NACA 4412 at 0^0 AoA..... | 25 |
| Figure 5.10 Pressure distribution of NACA 4412_1 at 0^0 AoA..... | 25 |
| Figure 5.11 Pressure distribution of NACA 4412_2 at 0^0 AoA..... | 25 |
| Figure 5.12 Velocity distribution of NACA 4412 at 0^0 AoA..... | 26 |
| Figure 5.13 Velocity distribution of NACA 4412_1 at 0^0 AoA..... | 26 |
| Figure 5.14 Velocity distribution of NACA 4412_2 at 0^0 AoA..... | 26 |
| Figure 5.15 Pressure distribution of NACA 4412 at 15^0 AoA..... | 25 |
| Figure 5.16 Pressure distribution of NACA 4412_1 at 15^0 AoA..... | 25 |

| | |
|---|----|
| Figure 5.17 Pressure distribution of NACA 4412_2 at 15 ⁰ AoA..... | 26 |
| Figure 5.18 Velocity distribution of NACA 4412 at 15 ⁰ AoA..... | 26 |
| Figure 5.19 Velocity distribution of NACA 4412_1 at 15 ⁰ AoA..... | 26 |
| Figure 5.20 Velocity distribution of NACA 4412_2 at 15 ⁰ AoA..... | 26 |
| Figure 5.21 Pressure distribution of NACA 4412 at 18 ⁰ AoA..... | 27 |
| Figure 5.22 Pressure distribution of NACA 4412_1 at 18 ⁰ AoA..... | 27 |
| Figure 5.23 Pressure distribution of NACA 4412_2 at 18 ⁰ AoA..... | 27 |
| Figure 5.24 Velocity distribution of NACA 4412 at 18 ⁰ AoA..... | 27 |
| Figure 5.25 Velocity distribution of NACA 4412_1 at 18 ⁰ AoA..... | 27 |
| Figure 5.26 Velocity distribution of NACA 4412_2 at 18 ⁰ AoA..... | 27 |
| Figure 5.27 Velocity vector of NACA 4412 at 0 ⁰ AoA..... | 28 |
| Figure 5.28 Velocity vector of NACA 4412_1 at 0 ⁰ AoA..... | 28 |
| Figure 5.29 Velocity vector of NACA 4412_2 at 0 ⁰ AoA..... | 28 |
| Figure 5.30 Velocity vector of NACA 4412 at 15 ⁰ AoA..... | 29 |
| Figure 5.31 Velocity vector of NACA 4412_1 at 15 ⁰ AoA..... | 29 |
| Figure 5.32 Velocity vector of NACA 4412_2 at 15 ⁰ AoA..... | 30 |
| Figure 5.33 Velocity vector of NACA 4412 at 18 ⁰ AoA..... | 30 |
| Figure 5.34 Velocity vector of NACA 4412_1 at 18 ⁰ AoA..... | 31 |
| Figure 5.35 Velocity vector of NACA 4412_2 at 18 ⁰ AoA..... | 31 |
| Figure 5.36 Turbulent viscosity of NACA 4412 at 18 ⁰ AoA..... | 32 |
| Figure 5.37 Turbulent viscosity of NACA 4412_1 at 18 ⁰ AoA..... | 32 |
| Figure 5.38 Turbulent viscosity of NACA 4412_2 at 18 ⁰ AoA..... | 33 |
| Figure 5.39 NACA 63-215 and improved airfoil NACA 63-215_1..... | 34 |
| Figure 5.40 Complete mesh..... | 34 |
| Figure 5.41 Enlarged view of NACA 63-215 and improved NACA 63-215_1 mesh..... | 34 |
| Figure 5.42 Lift coefficient at different AoA..... | 35 |
| Figure 5.43 Drag coefficient at different AoA..... | 36 |
| Figure 5.44 Cl/Cd at different AoA..... | 36 |
| Figure 5.45 Pressure distribution of NACA 63-215 at 0 ⁰ AoA..... | 37 |
| Figure 5.46 Pressure distribution of NACA 63-215_1 at 0 ⁰ AoA..... | 37 |
| Figure 5.47 Velocity distribution of NACA 63-215 at 0 ⁰ AoA..... | 37 |
| Figure 5.48 Velocity distribution of NACA 63-215_1 at 0 ⁰ AoA..... | 37 |
| Figure 5.49 Pressure distribution of NACA 63-215 at 17 ⁰ AoA..... | 38 |
| Figure 5.50 Pressure distribution of NACA 63-215_1 at 17 ⁰ AoA..... | 38 |
| Figure 5.51 Velocity distribution of NACA 63-215 at 17 ⁰ AoA..... | 38 |
| Figure 5.52 Velocity distribution of NACA 63-215_1 at 17 ⁰ AoA..... | 38 |

| | |
|---|----|
| Figure 5.53 Pressure distribution of NACA 63-215 at 21° AoA | 38 |
| Figure 5.54 Pressure distribution of NACA 63-215_1 at 21° AoA | 38 |
| Figure 5.55 Velocity distribution of NACA 63-215 at 21° AoA | 39 |
| Figure 5.56 Velocity distribution of NACA 63-215_1 at 21° AoA | 39 |
| Figure 5.57 Velocity vector of NACA 63-215 at 0° AoA..... | 39 |
| Figure 5.58 Velocity vector of NACA 63-215_1 at 0° AoA..... | 40 |
| Figure 5.59 Velocity vector of NACA 63-215 at 17° AoA | 40 |
| Figure 5.60 Velocity vector of NACA 63-215_1 at 17° AoA..... | 41 |
| Figure 5.61 Velocity vector of NACA 63-215 at 21° AoA..... | 41 |
| Figure 5.62 Velocity vector of NACA 63-215_1 at 21° AoA..... | 42 |
| Figure 5.63 Turbulent viscosity of NACA 63-215 at 17° AoA | 42 |
| Figure 5.64 Turbulent viscosity of NACA 63-215_1 at 17° AoA | 43 |
| Figure 7.1 Wing profile change mechanism | 46 |
| Figure 7.2. Usage of wing profile according to flight | 47 |

LIST OF SYMBOLS

| | |
|--------|--------------------------------|
| A.o.A. | Angle of attack |
| C | Chord Length (m) |
| C_D | Drag Coefficient |
| C_L | Lift Coefficient |
| F_D | Drag force |
| F_L | Lift force |
| K | Turbulence Kinetic Energy |
| Re | Reynolds Number |
| A | Surface Area (m ²) |
| q | Dynamic Pressure (Pa) |
| ρ | Density (kg/m ³) |
| μ | Dynamic Viscosity (kg/m-s) |

CHAPTER 1

INTRODUCTION

1.1 General Introduction

In the last decades, aviation sector is increasing and developing rapidly. Depending on these developments, aircraft performance and productivity are being increased by using new designs. For the aircraft productivity, aerodynamic performance is the most important parameter. The airfoils are the main effective parts of the aircrafts on the aerodynamic performance.

With the logic that can be associated with the working principle of the bird wings, airplane wings are the surfaces that the lift force affects on its and can be change shaped according to the aerodynamic performance by designers. In order for the aircraft continue to normal flight in the air, the weight of the plane must be balanced by the lifting force which is produced by the wings. It has been proven in tests and experiments that the producing drag force of the aircraft is related to the aircraft wings. (Lynch., 1982). Numerical methods (Finite element methods) are used to analyze the performance of the wings.

Finite element methods (FEM) are mostly used for designing of a new product or improving a recent product. There are many different finite element methods are developed for solution of solid mechanics problems and fluid mechanics problems. Computational fluid dynamics (CFD), which is a FEM tool, can be used for simulation of the airfoils.

An airplane wing has direct effects on most aerodynamic features. An example of these aerodynamic features is the approach and climb speed. Besides aerodynamic properties, it affects noise and emissions because the wings reduce propulsion. (Thibert et al., 1995).

Flow separation reduces aircraft wing performance to serious levels. Flow separation is a matter concerned with the design of the wing shape. There are some constraints in the military sector and aerodynamic designs have to be done considering these constraints. This necessity also brings with it some difficulties. These requirements are tried to be overcome by active and passive flow control systems (You and Moin, 2008).

Flow separation is very important phenomena for the aircrafts at climbing or descending stage. The viscous zone is visible even at very small angles, as the angle of attack increases, the separation of the boundary layers on the upper and lower surface of the wing increases. Result of this situation is that grow viscous region that leads to the decrease of lift (stall). This event adversely affects the lift force and drag force. This effect must be eliminated to increase performance and to decrease operating costs of the aircrafts. New airfoil concept which is worked about it could be extremely beneficial in making an aircraft more maneuverable by changing flow characteristics. Also, it increases the aerodynamic efficiency and therefore helps in improving the performance also.

1.2 Research Objectives and Tasks

In this thesis, the main purpose is to increase critical angle of attack values and decrease effect of flow separation by design an adjustable shape airfoil design. In this direction, the turbulence models, lift coefficient, drag coefficient, pressure and velocity contours, angle of attack have examined detailed. Research tasks can be order as follows:

- Reviewing research about stall, flow separation, and airfoil design in the literature.
- Definition and selection of the most suitable turbulence model
- Theory of fluid dynamics
- The description of the suitable mesh concentration
- CFD analysis of normal profile and adjustable New profile of NACA 4412 and NACA 63-215 airfoil using ANSYS FLUENT program (software).
- Checking the various Angle of attack
- Evaluate drag and lift coefficient

- Draw graphics and compare results

1.3 Layout of Thesis

A literature survey about stall, flow separation, and airfoil design is summarized in Chapter 2. General information about computational fluid dynamics is mentioned in Chapter 3. General information related with stall is summarized in Chapter 4. Adjustable airfoils is analyzed in Chapter 5. Results is considered in Chapter 6.



CHAPTER 2

LITERATURE REVIEW

Numerous researches have been done on flow separation related to the shape of the wing and which reduce the performance of the wing. Flow separation is regarded as an important problem in the aviation sector. Hence, passive and active flow control devices are improved to overcome this problem. Passive control devices, for example, vortex generators.

Jirasek (2005), explains in his study that the separation of flow is a delayable condition. Many flow control systems have been invented and tested to provide control of flow separation and increase lift. But most of these inventions were in fact difficult to implement.

Control of the flow separation by blowing and suction systems etc... different systems has been extensively investigated. Control devices involving zero-net-mass-flux oscillatory jets or synthetic jets have shown good feasibility for industrial applications and effectiveness in controlling flow separation (Glezer and Amitay, 2002; Findanis and Ahmed, 2008). The application of synthetic jets to flow separation control is based on their ability to stabilize the boundary layer by adding/removing momentum to/from the boundary layer with the formation of vortical structures.

In the literature, many different investigations are existing about the aerodynamic performance of the airfoils. General aerodynamic studies, active flow control studies and passive flow control studies are given in this chapter.

2.1. General aerodynamic studies

2.2. Active flow control studies

2.3. Passive flow control studies

2.1 General Aerodynamic Studies

Justin (2013) CFD analysis method preferred because CFD analysis gives faster and easier results than experimental works. This method gives certain results which are lift coefficient, drag coefficient, angle of attack, moment coefficient by using some basic parameters which are Reynolds number, angle of attack range, airfoil shape.

Kumar (2014) has done a detailed research on various airfoils and his aim is that research to effects of different airfoil shapes on drag and lift coefficient. The aircraft wings are the decisive factor in achieving sufficient drag force for movement of the aircraft whether in balance of aircraft weight and lift force. Angle of attack, critical angle of attack, lift and drift coefficients compared of asymmetric and symmetric airfoils which are using airfoil BOEING737, MIG21 and BELL 200XV. The lift coefficient and drag force is higher for the asymmetric airfoil whereas the stall angle is lower than the symmetrical airfoil.

Hossain et. al. (2014) used the cfd extension of the ansys program, which gives faster and more accurate results than the experimental ones. The Computational fluid dynamics identifies the flow with mathematical, numerical and software tools, evaluates these values in a virtual laboratory and gives results. In this study the results were obtained with the ANSYS program which is a computational analysis program. Result of this study is that best airfoil is the one with the highest lift to drag ratio.

Patel et. al. (2014) considered that if the attack angle is zero, there is no lift force and there is no change in the lift coefficient, in order to increase these values, the attack angle needs to increase. As the angle of attack increases, the drag force and drag coefficient increase, but this increase is less than the lift coefficient and lift force.

Kevadiya and Vaidya (2013) calculated lift and drag coefficient for naca 4412 for different angle of attacks. They used Sparat Almaras model for turbulence modelling which model solve an equation based kinematic viscosity. Result of their study that when angle of attacks increases until 8° Lift/Drag ratio increase, if the attack angle goes up 8° , the Lift/Drag ratio starts to decrease.

Mehmood et. al. (2012) analyzed the NACA0018 airfoil in different angle of attacks and different lengths to examine the use of the NACA0018 airfoil in the design of the diffuser. The researches reached that when angle of attack and length is increase also

velocity and drag increase. The other result there is always a fit between the maximum speed and the drag.

Sagat et. al. (2012) made CFD analyzes at the low Reynolds Number in this study, and compared these CFD analyzes results with experimental results. They studied the variation of the pressure coefficient at the lower and upper surfaces of the airfoil at different angle of attacks 0° to 10° . According the results of this study upper surface has lower negative coefficients of pressure at higher angles of attack and lower surface has lower negative coefficients of pressure at lower angles of attack. The lift coefficient, drag coefficient and the velocity distribution of the air passing over airfoil is depends on pressure distribution.

Panda (2015) wanted to calculate the aerodynamic coefficients and examine the flow behavior on the airfoil surface at high Reynolds Numbers and different angle of attacks -5° to 25° . NACA 2314 wing were analyzed using the software ANSYS 15.0 program for calculate the pressure coefficient, lift coefficient and draw L/D graph. Lift increases up to a certain point, which is the maximum of lifting from -5 to 20 degrees angle of attacks. If the uphill continues, the drag becomes more dominant and the aircraft enters the stall zone.

Kevadiya (2013) considered variation pressure coefficient of NACA 4412. He is study CFD method in his study. As a result of the CFD analysis, when the attack angle was 0 degree, the pressure coefficient at the top of the airfoil was negative. When the attack angle is increased regularly, it is observed that the pressure coefficient in the upper surface is decreased, the pressure coefficient in the lower surface is increased and the maximum pressure coefficient in the lower surface is 12 degree.

Kostića and Rašuo (2016) investigated the effects of the critical angle of attacks on the aircraft during flight. He concluded that as a result of his work, the movement of the aircraft in the critical angle of attack is directly related to the airfoil shape and defined specification of flow.

Dash (2016) analyzed the aerodynamic properties of the NACA0012 airfoil in the constant reynolds number. He has made a number of assumptions in their work, one of which is the acceptance of NACA0012 as a wind tunnel blade. He used the ANSYS program in his analysis to examine the airfoil at different attack angles which are 4 , 6 ,

8, 10 degree. If we compare the bottom and upper surface of airfoil we can see that velocity of upper surface higher than bottom surface and pressure coefficient is negative for upper surface, positive for bottom surface. When we view the results we can say that while angle of attack is increase also lift coefficient increase.

2.2 Active Flow Control Studies

Demir et. al. (2016) explained the flow control methods in their study and differences between them also discussed the numerical examination on NACA4412 on different angle of attacks. These flow control methods are divided into two types active and passive flow control. Active flow energies result by adding energy to the direct boundary layer, passive flow control method can be executed by adding geometrical interruptions. Using these methods, it is possible to make the stall event happen at higher angle of attacks also the amount of increase and decrease in lift and drag can be controlled.

Milano et. al. (2000) goal in his study is that solve the active control problem with using two system optimizers to reduce the active control system problem, and the drag with these optimizers was reduced by up to 60 percent. They used two methods to reduce dragging; the use of systems delaying flow separation and the use of mechanisms to provide modification of vortices at separation points.

Tuck and Soria (2004) examined aerodynamic specifications by placed a device zero net mass flux (ZNMF) which is active flow control device in leading edge of NACA0015. They chose active flow control which defines energy expenditure in their work because he said that the greatest advantage of active flow control versus passive flow control is to turn the active control device on and off when they want. As a result according to the optimum forcing frequency values taken from the ZNMF, the airfoil stall angle was reduced from 10° to 18° .

Goodarzi et. al. (2012) presented the results of different angle of attacks in his work which is based active flow control method by placing a blowing jet over Naca0015 airfoil. He used the Sparse Allmaras turbulence model in his studies and used CFD fluent to solve these equations. It is seen that the blowing is affected lift force and drag force directly, and the result is that the lift force is increased and the drag force is lowered.

Singh et. al. (2016) profited by synthetic and continuous jets to investigate the aerodynamic properties of NACA23012 using the CFD active flow control method. Researchers placed combined jet at the 12% chord length where the flow separation begins and all necessary values are obtained using the simulation of Sparse Allmaras turbulence model. As a result, they have proven that if the most appropriate values are selected, efficiency is seriously increase. When free stream velocity is $R=1$ the lift is obtained 92% and $R=0$ 68% at angle of attack 22° also while the stall angle of the used airfoil model is normally calculated as 16° , the stall angle with optimal values is delayed by 20° .

2.3 Passive Flow Control Studies

Hocine Tebbiche and Mohammed S. Boutoudj (2015) were used passive vortex generators which caused momentum to flow into the boundary layer and caused the flow separation to be delayed or not occurs completely. The main purpose of this study is that increase the aerodynamic performance by placing passive vortex generators which has delta shape at the point where begins the separation of the naca4412 airfoil. Passive flow control method was preferred by researches due to geometric discontinuities of airfoil. They eventually achieved a 20% increase in lift and announced that they were able to delay the fall of the airfoil to stall status.

Shehata et. al. (2017) applied the passive flow control method to make aerodynamically more stable airfoil with symmetrical profiles in the stall zone. They aimed to increase the aerodynamic performance of the symmetrical airfoil by using blowing or suction methods with the help of Well turbine blades and by applying a passive flow control method on stall conditions. They used the symmetric NACA profile in this study, and they preferred CFD. They created an opening in the airfoil, claiming that this openness simulates the suction effect. It was observed that this openness 53% increased the torque coefficient in stall region and delayed the stall. The most important factor for delaying flow separation is increase the lifting and at the same time reduce the drag.

Gopinathan and Ganesh (2015) investigated the control of the flow separation of NACA0015 airfoil with the help of vortex generators. They used the Sparat Allmaras turbulence model in their investigations and solved the equations with the help of FLUENT. It has been observed that there is no effect of vortex generators on airfoils

with low attack angle. When the attack angle is 14, it is observed that the lifting coefficient decreases rapidly and the drag coefficient increases seriously. This situation is a cause for stall for normal airfoil. The stall region Angle of attack is 16 for airfoils which have vorteks generators. These results suggest that vortex generators have a significant effect on delaying the stall.

Mashud and Ferdous (2012) worked on the effect of flow separation of a vortex cavity formed on the upper surface of the airfoil. The angle of attack is directly proportional to the flow separation, when angle of attack is increased also flow separation increase. As a result of their investigations, it has been determined that the most efficient angle of attack values 8° and 11° for control flow separation by vortex cavity. It has been observed that the vortex cavity has no effect on flow separation for the angle of attack above 12° .

CHAPTER 3

COMPUTATIONAL FLUID DYNAMICS

Computational Fluid Dynamics (CFD) is a computer-aided fluid analysis method where all the calculations are made in details, and the flow field and physical details are visually displayed. In the other words CFD is a method which is making a numerical analysis with fluid mechanics parameters by help of computer software Figure 3.1.

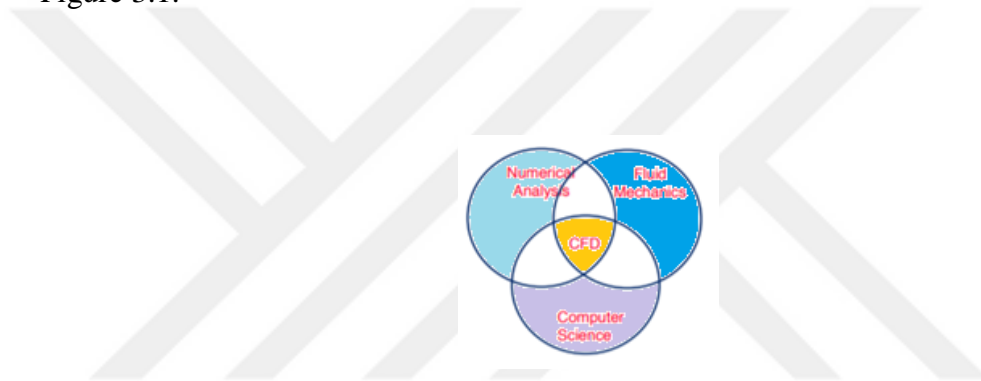


Figure 3.1 Computational fluid dynamics

With the CFD method, the designer easily simulates the different conditions and obtain results quickly. Without production, it is possible that systems can be tested with this method. This is a significant advantage in reducing costs. We can explain the CFD process sequence as follows: first, the definition of the fluid problem must be fully defined, then the physical properties of the fluid are determined, and these determined physical properties are transformed into the mathematical formulas we call Navier Stokes equations.

3.1 Navier-Stokes Equations

Navier-Stokes equations are basic partial differential equations which define the flow of incompressible fluids. These equations are based the conservation law, energy equations, continuity equations and energy equations.

Conservation Law;

The protection law states that a measurable value which are mass, energy, momentum etc... within an isolated system does not change over time.

$$\frac{dX}{dt} = X_{in} - X_{out} = 0 \quad (3.1)$$

Where X is a measurable value.

So, we can say that X value is constant as a result of the above equation.

Continuity equation defined as;

$$\frac{D\rho}{Dt} + \rho \frac{\partial U_i}{\partial x_i} = 0 \quad (3.2)$$

Momentum equation is also defined as;

$$\rho \frac{\partial U_j}{\partial t} + \rho U_i \frac{\partial U_j}{\partial x_i} = -\frac{\partial P}{\partial x_j} + \lambda \frac{\partial \tau_{ij}}{\partial x_i^2} - \tau_{ij} \frac{\partial U_j}{\partial x_i} + \rho g_j \quad (3.3)$$

$$\tau_{ij} = \mu \left(\frac{\partial U_j}{\partial x_i} + \frac{\partial U_i}{\partial x_j} \right) + \frac{2}{3} \delta_{ij} \mu \frac{\partial U_k}{\partial x_k} \quad (3.4)$$

Energy equation;

$$\rho c_\mu \frac{\partial T}{\partial t} + \rho c_\mu U_i \frac{\partial T}{\partial x_i} = -P \frac{\partial U_i}{\partial x_i} + \lambda \frac{\partial^2 T}{\partial x_i^2} - \tau_{ij} \frac{\partial U_j}{\partial x_i} \quad (3.5)$$

If we write simplify form of Navier Stokes Equation:

$$\frac{\partial(\rho\Phi)}{\partial t} + \frac{\partial}{\partial x_i} (\rho U_i \Phi - \Gamma_\Phi \frac{\partial \Phi}{\partial x_i}) = \rho\Phi \quad (3.6)$$

Continuous energy and moment equations can be obtained when the necessary values are given to the Φ variable. (For example, $\Phi = 1, U_j, T$)

3.2 Finite Element Methods

In order for Navier Stoke equations to be solved on a computer, we need to translate it into a form that the computer can be solve, name of this form is discretized form. We use finite element methods for our study as a discretized method.

Finite Element Analysis, expressed as a mathematical a physical system. This system is a sub-segment separable model with material properties and applicable boundary conditions. The basis of the FEA, the complex region is divided into simple geometric subregions known as end elements (**Figure 3.2**). Average of the results obtained for each node in these sub-regions is accepted as the correct result.

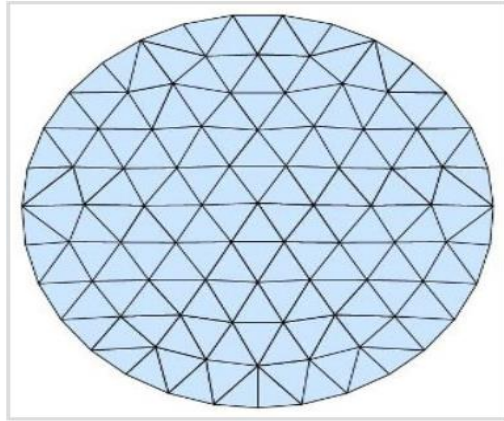


Figure 3.2 Divided domain

Each grid of divided area must be capable of adequately describing the properties of flow.

3.3 ANSYS Software

ANSYS software is a computer program that can be modeled and simulated fluid systems and can achieve the desired result with the interactions.

CFD fluent chart in ANSYS is,

- Geometry Design
- Mesh Generation
- Setup
- Solution
- Results

Firstly, two or three-dimensional design of complex fluid systems is required depending on the problem. For geometric design, the ANSYS has a toolbox which name is the geometric design. Also, the design domain in which the complex flow analysis is represented in the Figure 3.3.

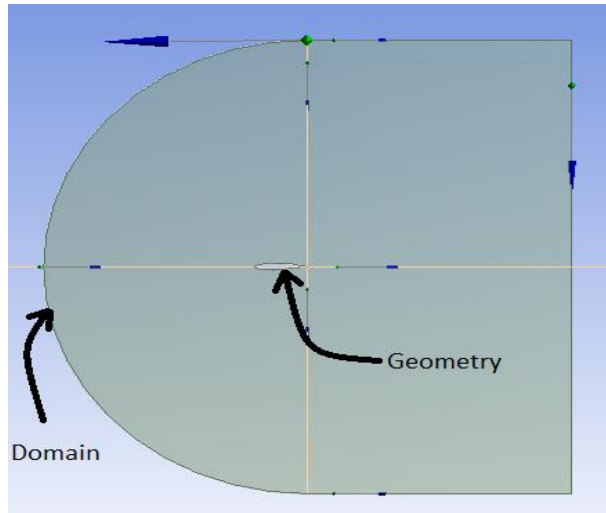


Figure 3.3 Design domain

ANSYS is based on the finite element method, it helps to calculate the flow equations on each mesh which is obtained from design domain in Figure 3.4.

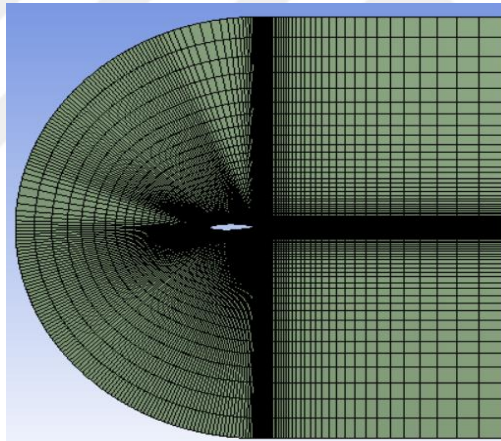


Figure 3.4 Mesh model

After the modeling the design domain and mesh model, flow parameters related to the flow system such as flow regime modeling, boundary conditions are defined (in **Figure 3.5**) and the analysis settings are completed. After definitions are finished, analysis can be performed.

| | |
|-----------------------|------------------------------------|
| airfoil_wall | Multiphase - Off |
| inlet | Energy - Off |
| interior-surface_body | Viscous - Spalart-Allmaras (1 eqn) |
| outlet | Radiation - Off |
| wall | Heat Exchanger - Off |
| wall-surface_body | Species - Off |
| | Discrete Phase - Off |
| | Solidification & Melting - Off |
| | Acoustics - Off |
| | Electric Potential - Off |

Figure 3.5 Setup-boundary conditions

After analysis is converged, pressure distribution, velocity distribution, lift coefficient value, drag coefficient value, moment coefficient value and etc. can be represented as a listed, contours, vectors and graphically using tool box in Figure 3.6.

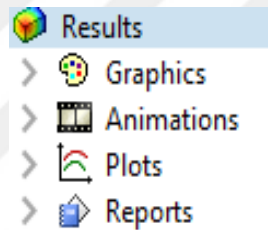


Figure 3.6 Results tool box

CHAPTER 4

STALL

When aircraft is exceed specified critical angle of attack ,it can not produce the required lift force for normal flight and falls into air space.This situation is called stall in aviation.There is a few cause of stall.Another cause is that aircrafts have a special speed for its holding in air,if speed of aircraft drops below this speed the lift force generated by the airfoil of aircraft cannot carry the weight of aircraft and this situation also caused the stall.The most dangerous situation for an aircraft by aviation authorities is considered Stall Figure 4.1 .

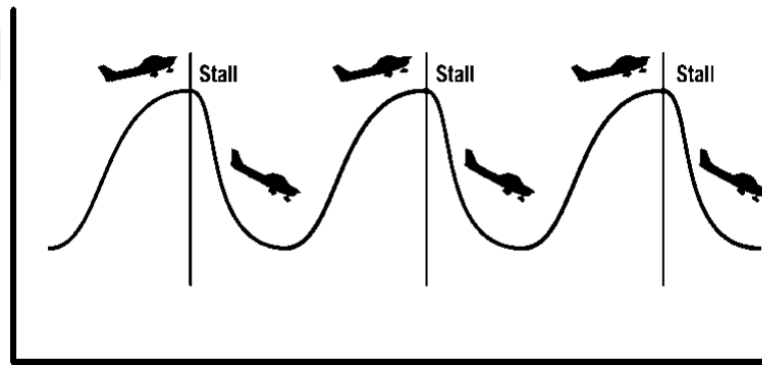


Figure 4.1 Stall situation

The critical attack angle depends on the shape of the airfoil, the aspect ratio airfoil etc. Maximum lift coefficient occurs at critical angle of attack Figure 4.2.

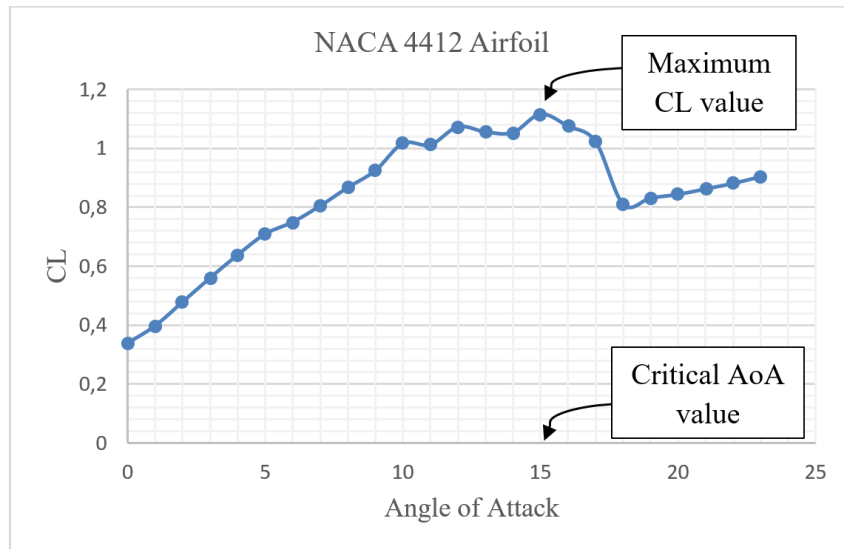


Figure 4.2 Critic angle of attack & maximum lift coefficient

4.1 Flow Separation

Flow separation which starts even at very small angles on the airfoil surface reaches a level that affects the lifting force of the airplanes with the increase of attack angle. When the separation of the flow increases, the flow separation reaches such a point that the lift force is lower than the drag force and stall occurs after all of them.

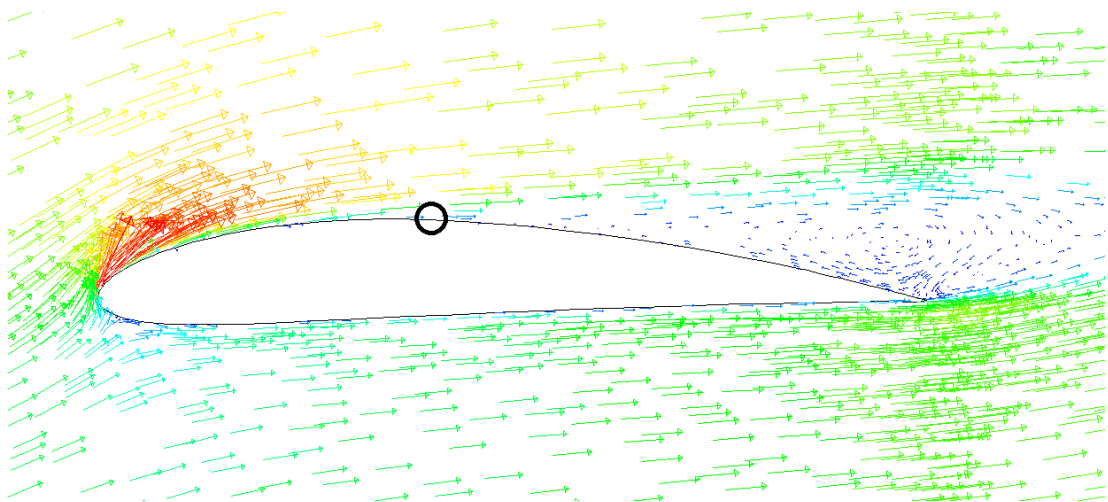


Figure 4.3 Flow separation

Another important effect that causes flow separation is reverse pressure gradient. When the boundary layer moves against the negative pressure gradient, flow separation occurs. The speed decreases with increasing pressure in the flow direction. By continuing these conditions, the velocity of the boundary layer approaches zero and at

the end the velocity becomes zero and the flow is separated from the surface. As the speed drops, there is an extreme momentum loss near the wall, and there is a flow separation in a boundary layer (negative pressure gradient) that tries to move downwards against increasing pressure. Drag force increases as a result of separation of boundary layer.

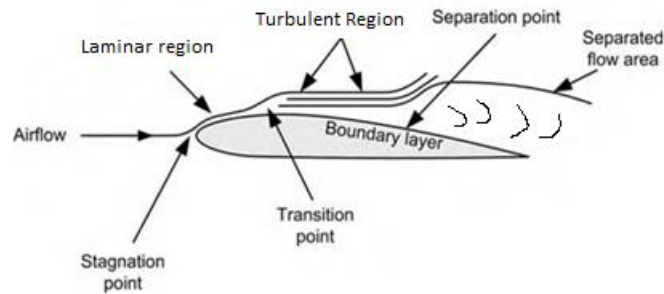


Figure 4.4 Schematic flow separation

4.2 Stall Warning Systems

With the development of the aerospace industry, flow control systems have been developed that increase lift, reduce drag, and reduce noise levels. These flow control systems are divided into active control systems and passive control systems. Passive control systems are based on geometric shapes and active control systems are systems based on adding energy and momentum.

Stall is a very dangerous situation in terms of flight comfort and flight safety. The pilot can take precautions against the stall if it is notified in advance. Scientists have developed warning systems that alert pilots before they fall into this situation Figure 4.5.

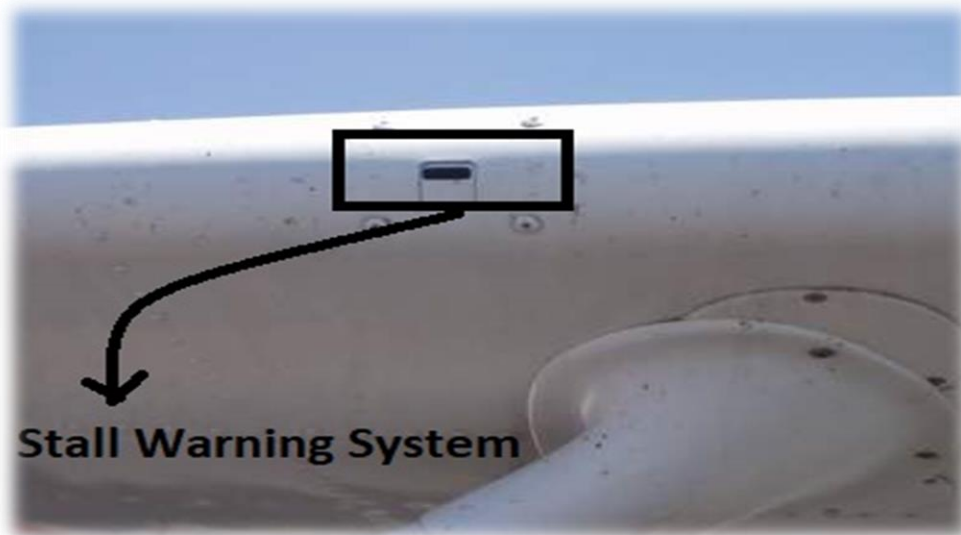


Figure 4.5 Stall warning system

We can categorized stall warnig sytems as;

- Pre-Stall Buffet Pre-Stall Buffet is a system that aerodynamic buffets alert the smooth flow on the upper surface of the aircraft wing to turn into turbulence flow.
- Audible Warning system is a system that gives audible alert when an electronic or mechanical device approaches stall speed.
- Stick Shakeris a system which occurs two mechanical systems which are stick pusher and stick shaker. Stick shaker actives before pusher for ensuring prevent the stall situation
- Angle of Attack this system refers to a system that gives various warnings and signals when the aircraft is over the predetermined angle of attack.

CHAPTER 5

CASE STUDIES OF ADJUSTABLE AIRFOIL DESIGN

5.1 Introduction

A wing is a surface used to produce an aerodynamic force (Figure1) normal to the direction of motion by traveling in air or another gaseous medium. A wing is an extremely efficient device for generating lift. Its aerodynamic quality, expressed as a Lift-to-drag ratio, can be up to 60 on some gliders and even more. This means that a significantly smaller thrust force can be applied to propel the wing through the air in order to obtain a specified lift (Chitte et. al., 2013).

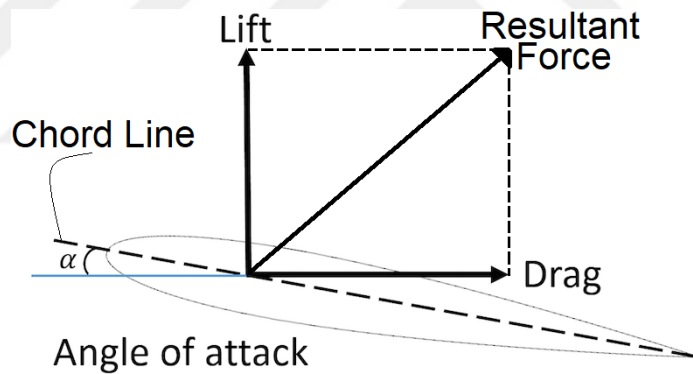


Figure 5.1 Lift force, drag force and angle of attack

The performance of an airplane wing is often degraded by flow separation (Stall). Flow separation on an airfoil surface is related to the aerodynamic design of the airfoil. Hence in the literature many different studies are exist about the investigation of aerodynamic performance of airfoils.

Usage of computational fluid dynamics (CFD) tools by the aerospace field to increase understanding of fluid dynamic and aerodynamic phenomena has been rapidly increasing during the past decade. Also, numerical simulation has become a

significant and growing aspect of the aircraft design process. Thanks to CFD, dependency on wind tunnel investigations are reduced so consequently design cost is also reduced. As a result of these developments, wing performances are increased using the CFD tools (Holst, 1994).

Aerodynamic database was developed for airfoils and wings at stall and post-stall AoA. Detailed results for three different airfoils were presented to compare their stall and post-stall behavior. The results for finite wings at stall and post-stall conditions focused on the effects of taper-ratio and sweep angle, with particular attention to whether the sectional flows can be approximated using two-dimensional flow over a stalled airfoil (Justin et. al., 2013).

Pressure distribution over the airfoils were analyzed at different AoA. The pressure distributions as well as coefficient of lift to coefficient of drag ratio of two airfoils were visualized and compared (Hossain et. al., 2014).

The lift coefficient of a fixed-wing aircraft can vary with changing AoA. Increasing AoA was associated with increasing lift coefficient up to the maximum lift coefficient, after which lift coefficient decreases. Numerical and experimental investigation was performed to obtain the lift and the drag forces.

5.2 Analysis

The performance of an airplane wing has a significant effect on the runway distance, approach speed, climb rate, payload capacity, and operation range, but also on the community noise and emission level as an efficient lift system also reduces thrust requirements (Thibert et. al., 2014).

Angle of Attack (AoA) is the angle between the oncoming air or relative wind and a reference line (chord line) on the airplane or wing (Figure5.1). This angle effects the aerodynamic forces lift and drag. Area A in equation 1 increases with increasing AoA value. The drag force F_D is given equation (5.1).

$$F_D = \frac{1}{2} \rho v^2 C_D A \quad (5.1)$$

where ρ is density, v is the velocity and A is the area. So, coefficient of drag C_D is given by the equation (5.2).

$$C_D = \frac{F_D}{\frac{1}{2}\rho v^2 A} \quad (5.2)$$

The lift force F_L is given equation (5.3).

$$F_L = \frac{1}{2}\rho v^2 C_L A \quad (5.3)$$

coefficient of drag C_L is given by the equation (5.4).

$$C_L = \frac{F_L}{\frac{1}{2}\rho v^2 A} \quad (5.4)$$

Before starting the analyzes, in order to confirm the correctness of mesh structure and determine the most suitable number of elements, mesh structures were formed by different element numbers and results of drag coefficient and lift coefficient were given in figure 5.2. According to these results if using 30000 elements in the analyzes, we can to obtain sufficient sensitivity in the results. The information given above was obtained as a result of examination of NACA 4412 airfoil.

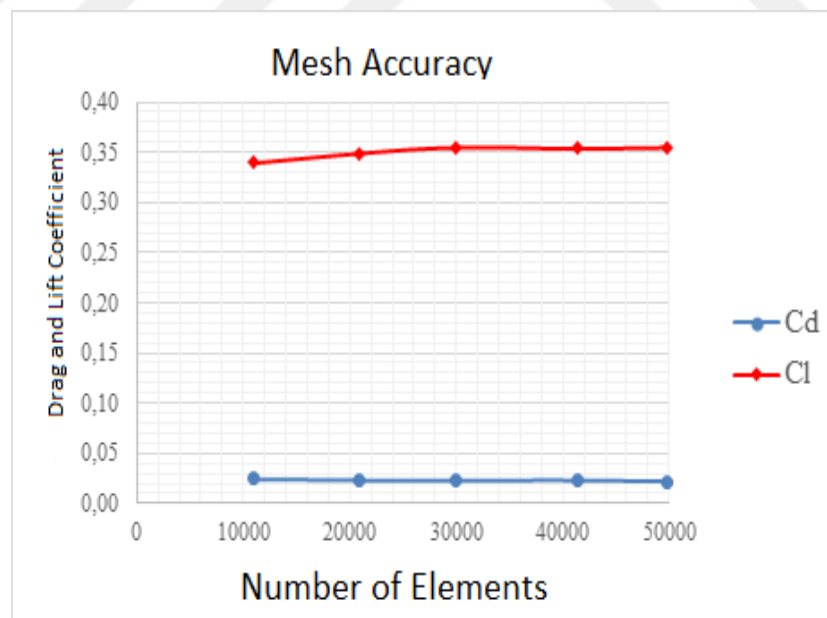


Figure 5.2 Mesh accuracy

In this study, CFD analysis was carried out in different angles and different profiles. Analysis parameters are listed in the table 5.1.

Table 5. 1 Analysis parameters

| | |
|------------------------------|-----------------------------|
| Node | 30272 |
| Elements | 29920 |
| Solver | Pressure based steady state |
| Viscous model | Spalart-Allmaras |
| Density (kg/m ³) | 1.225 |
| Turbulent viscosity | 1 |
| Inlet velocity (m/s) | 1 |
| Chord-length (m) | 1 |
| Momentum | Second order upwind |

5.3 Adjustable NACA 4412 Profile Design

Aerodynamic efficiency of wind turbine was investigated. NACA 4412 airfoil was considered for analysis of wind turbine blade at various angles of attack (AoA) from 0° to 12°. The coefficient of lift and drag values were calculated for $7,0388 \times 10^4$ Reynolds number (Kevadiya and Vaidya, 2013).

The computational fluid dynamic (CFD) analysis was used to determine the aerodynamic performance of two-dimensional (2D) flow over airfoils. In this section, aerodynamic performance of the NACA 4412 and 2 improved NACA 4412 airfoil (Figure 5.3) was compared. Aerodynamic performance of these 3-airfoils was compared at different AoA (between 0° and 23°) values. Drag coefficient, lift coefficient and flow separation were used as performance parameter.

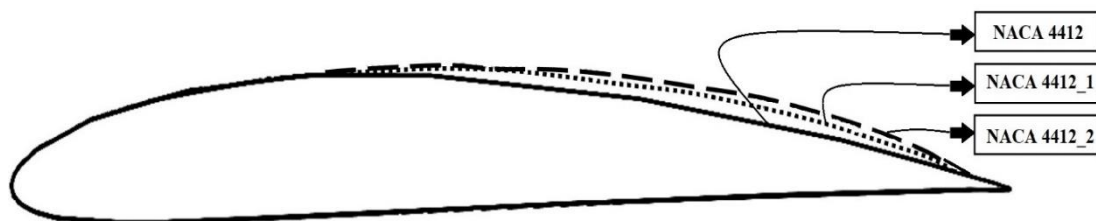


Figure 5.3 NACA 4412 and 2 improved Airfoils

Analysis were performed using CFD tool of ANSYS, which is commercial finite element analysis program. Complete mesh distribution can be seen in the figure 5.4,

enlarged view of NACA 4412 mesh and enlarged view of 2 improved NACA 4412 mesh is given in the figure 5. 5.

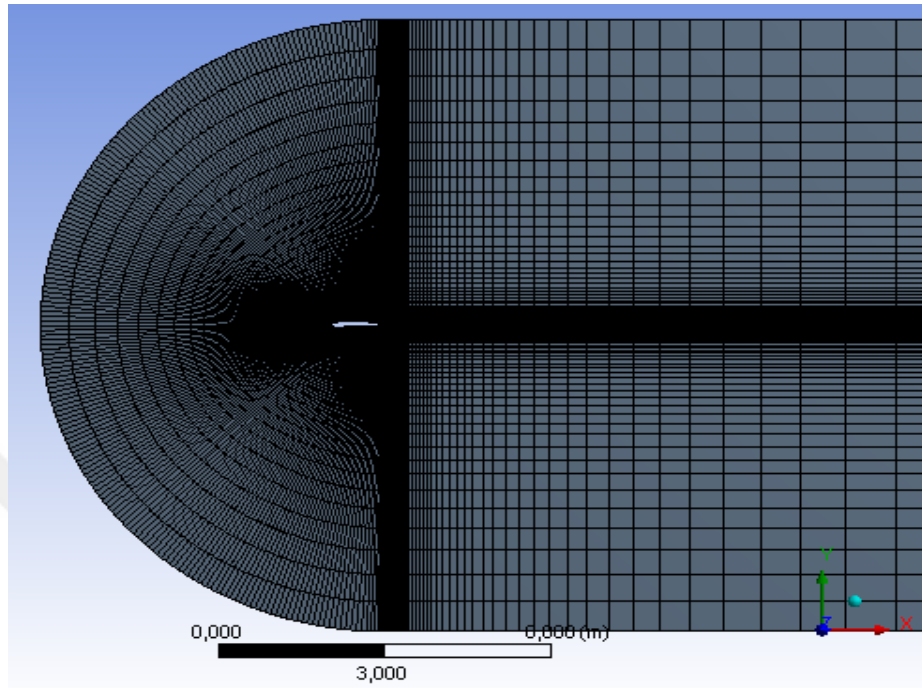
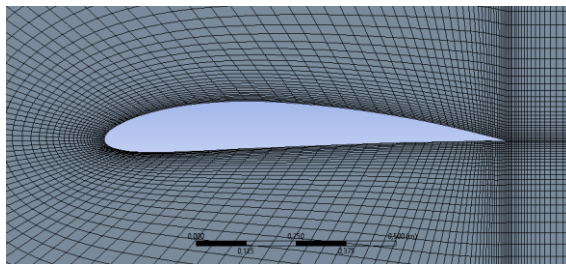
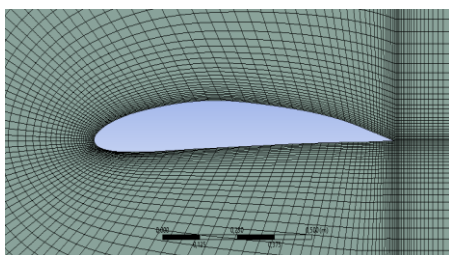


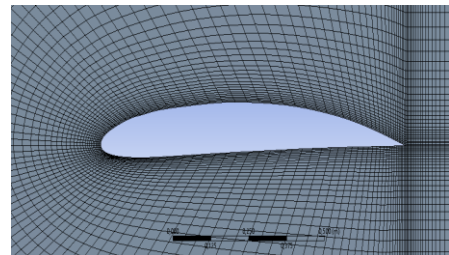
Figure 5.4 Complete mesh



a) NACA 4412



b) NACA 4412_1



c) NACA 4412_2

Figure 5.5 Enlarged view of NACA 4412 and improved NACA 4412 mesh

Lift coefficients of NACA 4412, NACA 4412_1, and NACA 4412_2 at different AoA were given in the figure 5.6. Also, drag coefficients of NACA 4412, NACA 4412_1, and NACA 4412_2 at different AoA were given in the figure 5.7.

When figure 5.6 was investigated, it was seen that maximum lift coefficient was obtained at 15° AoA for original NACA 4412 and minimum lift coefficient was obtained at 0° AoA for original NACA 4412. Also, maximum lift coefficient loss was occurred at 18° AoA due to flow separation. So, comparisons of the results were given at these 3 angles of attack values.

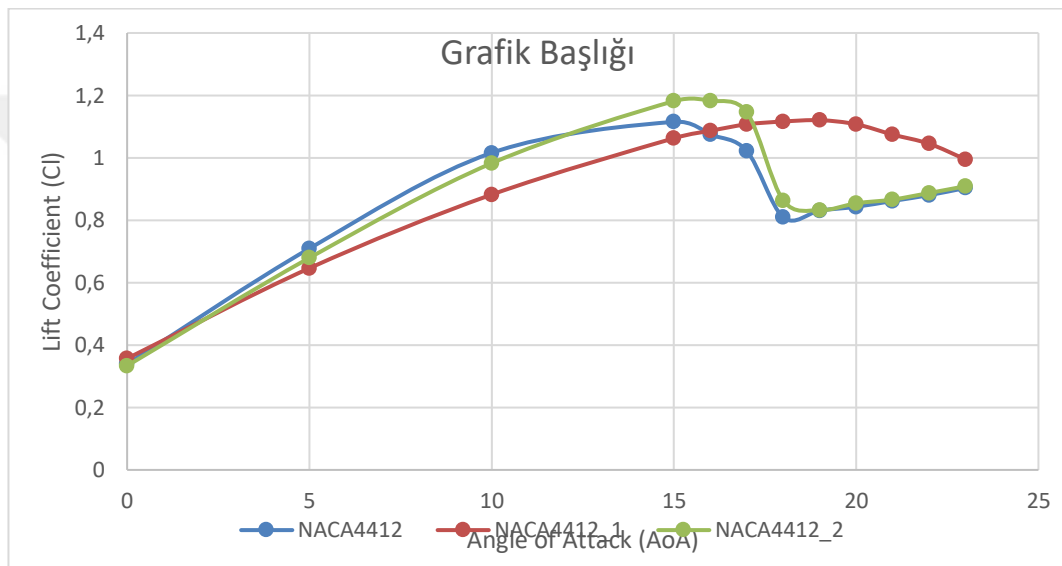


Figure 5.6 Lift coefficient at different AoA

The NACA 4412 airfoil must be used up to a 12 degree, NACA 4412_2 must be used up between 12 and 17 degrees and NACA 4412_1 must be used up after 17-degree angle of attack, to obtain maximum lift.

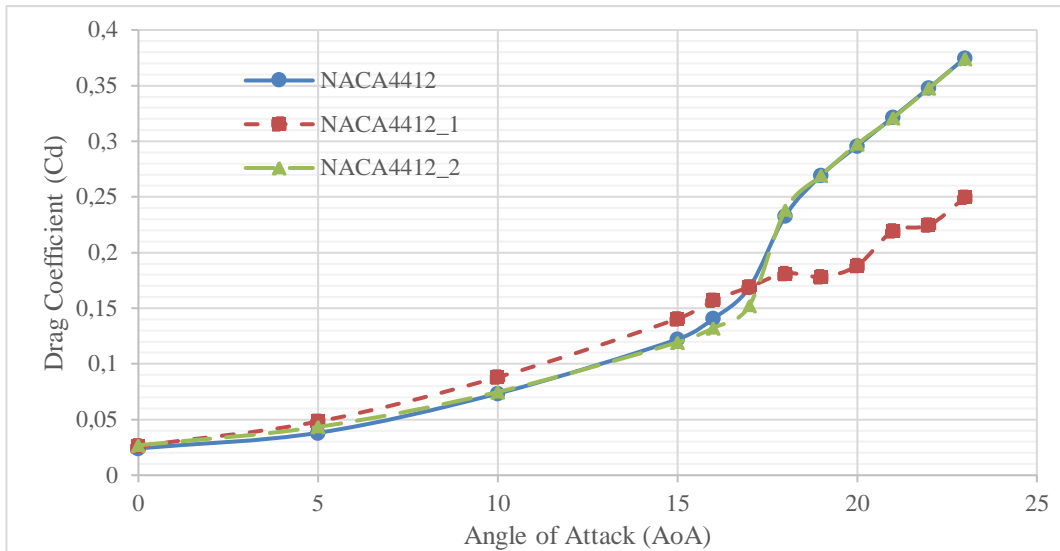


Figure 5.7 Drag coefficient at different AoA

The NACA 4412 and NACA 4412_2 airfoil must be used up to a 17 degree and NACA 4412_1 must be used up after 17-degree angle of attack, to obtain minimum drag.

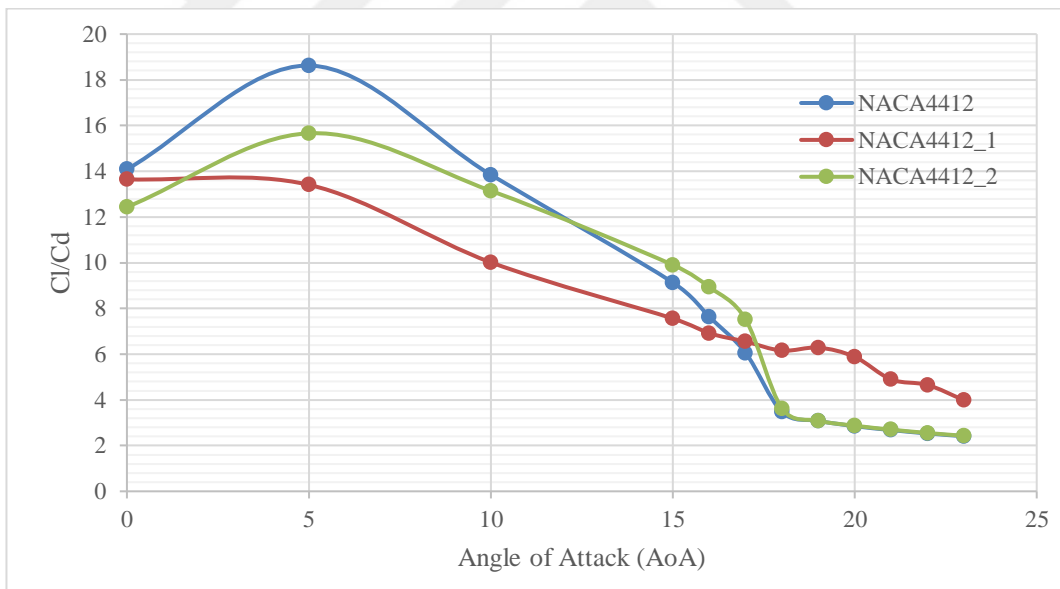


Figure 5.8 Cl/Cd at different AoA

The NACA 4412 airfoil must be used up to a 12 degree, NACA 4412_2 must be used up between 12 and 17 degrees and NACA 4412_1 must be used up after 17-degree angle of attack, to obtain maximum aerodynamic efficiency. Cl/Cd ratio was given according to angle of attack in the figure 5.8.

Pressure distribution of NACA 4412, NACA 4412_1, and NACA 4412_2 at 0° AoA value were given in the figure 5.9, 5.10 and 5.11 respectively. Velocity distribution of NACA 4412, NACA 4412_1, and NACA 4412_2 at 0° AoA value were given in the figure 5.12, 5.13, and 5.14 respectively.

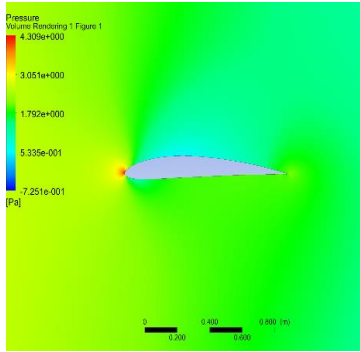


Figure 5.9 Pressure distribution of NACA 4412 at 0° AoA

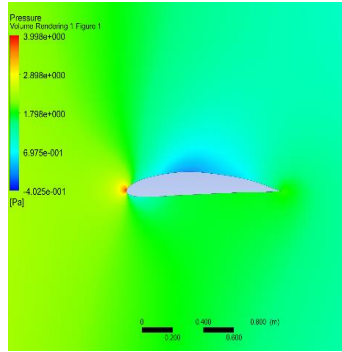


Figure 5.10 Pressure distribution of NACA 4412_1 at 0° AoA

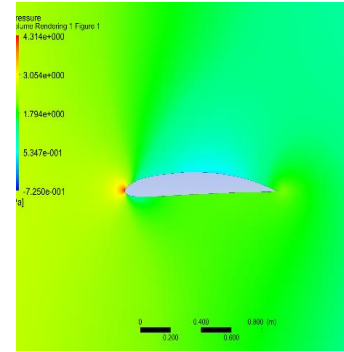


Figure 5.11 Pressure distribution of NACA 4412_2 at 0° AoA

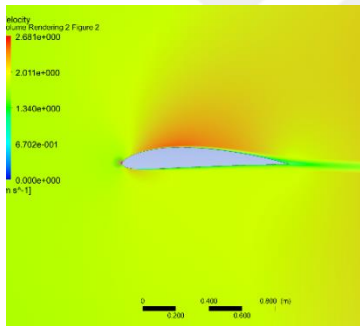


Figure 5.12 Velocity distribution of NACA 4412 at 0° AoA

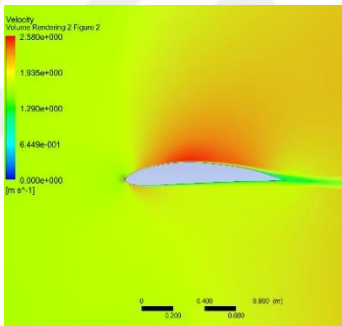


Figure 5.13 Velocity distribution of NACA 4412_1 at 0° AoA

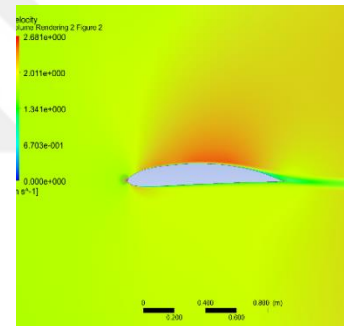


Figure 5.14 Velocity distribution of NACA 4412_2 at 0° AoA

Pressure distribution of NACA 4412, NACA 4412_1, and NACA 4412_2 at 15° AoA value were given in the figure 5.15, 5.16 and 5.17 respectively. Velocity distribution of NACA 4412, NACA 4412_1, and NACA 4412_2 at 15° AoA value were given in the figure 5.18, 5.19, and 5.20 respectively.

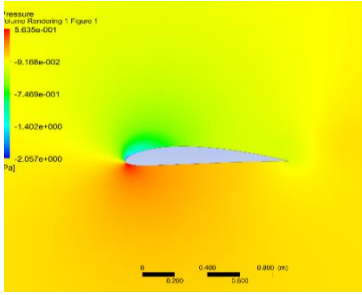


Figure 5.15 Pressure distribution of NACA 4412 at 15⁰ AoA

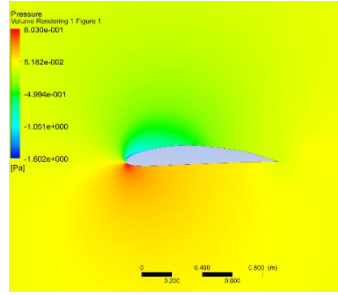


Figure 5.16 Pressure distribution of NACA 4412_1 at 15⁰ AoA

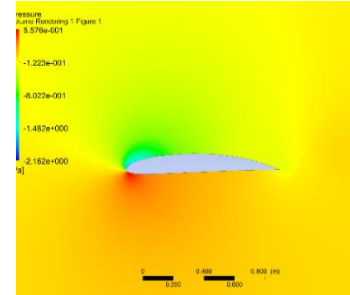


Figure 5.17 Pressure distribution of NACA 4412_2 at 15⁰ AoA

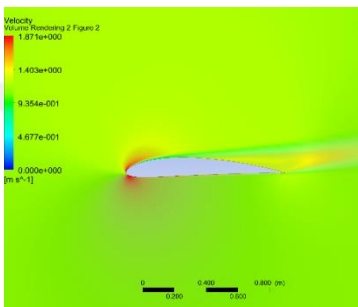


Figure 5.18 Velocity distribution of NACA 4412 at 15⁰ AoA

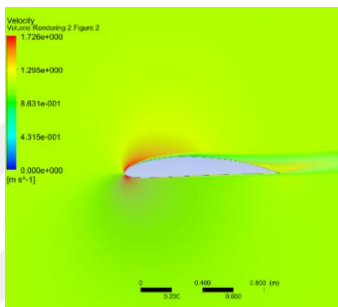


Figure 5.19 Velocity distribution of NACA 4412_1 at 15⁰ AoA

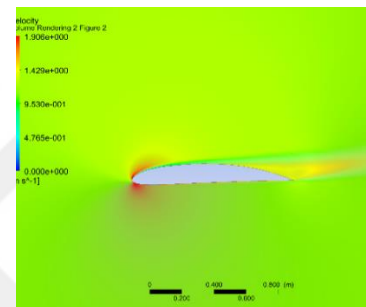


Figure 5.20 Velocity distribution of NACA 4412_2 at 15⁰ AoA

Pressure distribution of NACA 4412, NACA 4412_1, and NACA 4412_2 at 18⁰ AoA value were given in the figure 21, 22 and 23 respectively. Velocity distribution of NACA 4412, NACA 4412_1, and NACA 4412_2 at 18⁰ AoA value were given in the figure 5.24, 5.25, and 5.26 respectively.

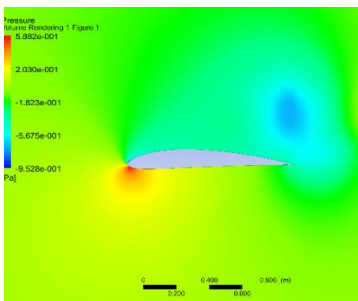


Figure 5.21 Pressure distribution of NACA 4412 at 18⁰ AoA

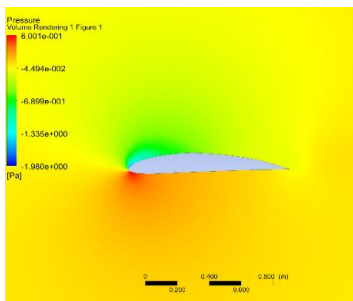


Figure 5.22 Pressure distribution of NACA 4412_1 at 18⁰ AoA

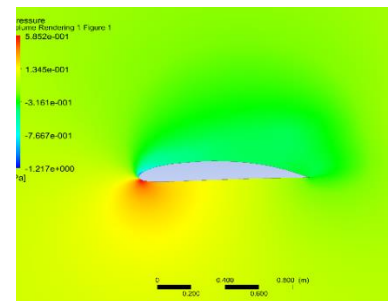


Figure 5.23 Pressure distribution of NACA 4412_2 at 18⁰ AoA

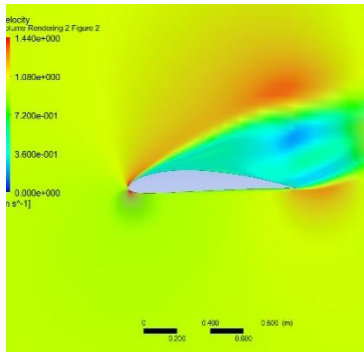


Figure 5.24 Velocity distribution of NACA 4412 at 18° AoA

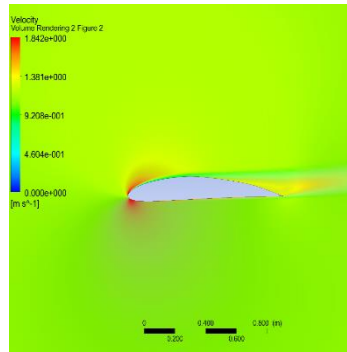


Figure 5.25 Velocity distribution of NACA 4412_1 at 18° AoA

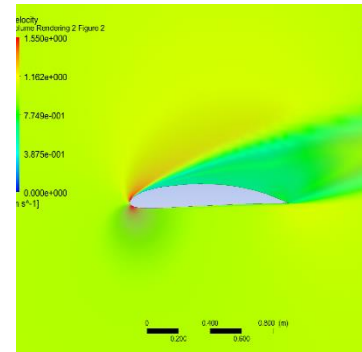


Figure 5.26 Velocity distribution of NACA 4412_2 at 18° AoA

Velocity vector of NACA 4412, NACA 4412_1, and NACA 4412_2 at 0° AoA value were given in the figure 5.27, 5.28, and 5.29 respectively.

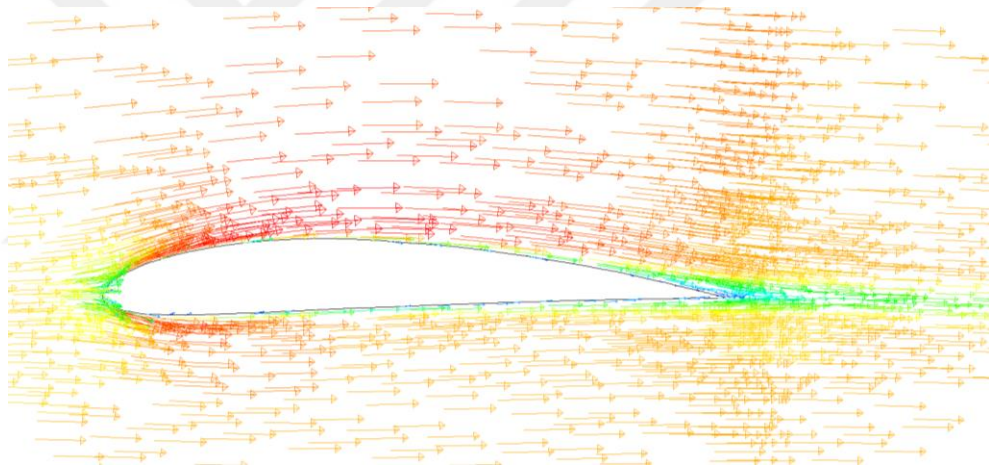


Figure 5.27 Velocity vector of NACA 4412 at 0° AoA

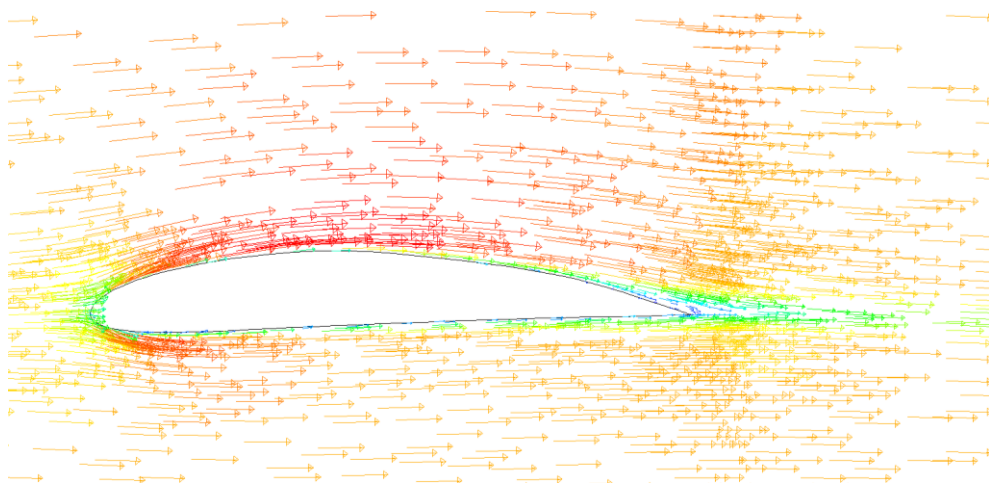


Figure 5.28 Velocity vector of NACA 4412_1 at 0° AoA

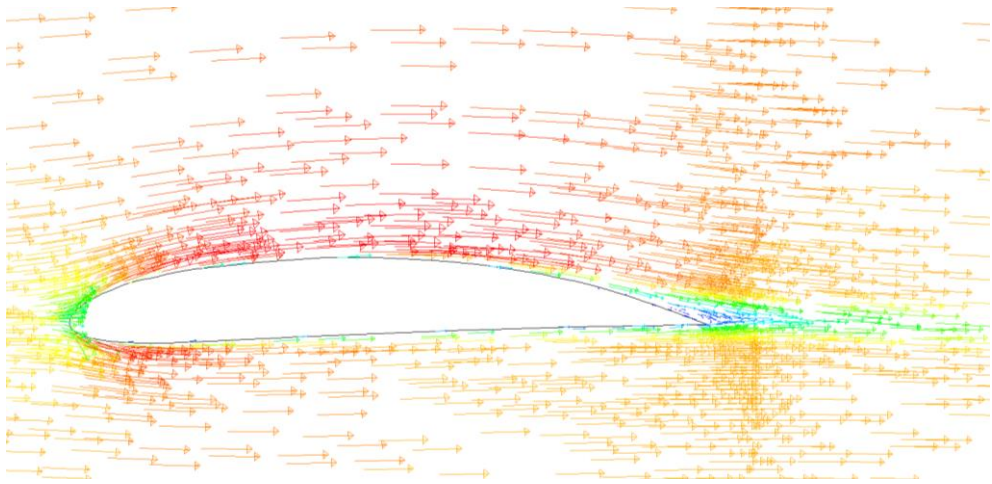


Figure 5.29 Velocity vector of NACA 4412_2 at 0° AoA

When the figure 5.27, 5.28, and 5.29 were investigated it was seen that there was no flow separation at 0° AoA.

Velocity vector of NACA 4412, NACA 4412_1, and NACA 4412_2 at 15° AoA value were given in the figure 5.30, 5.31, and 5.32 respectively.

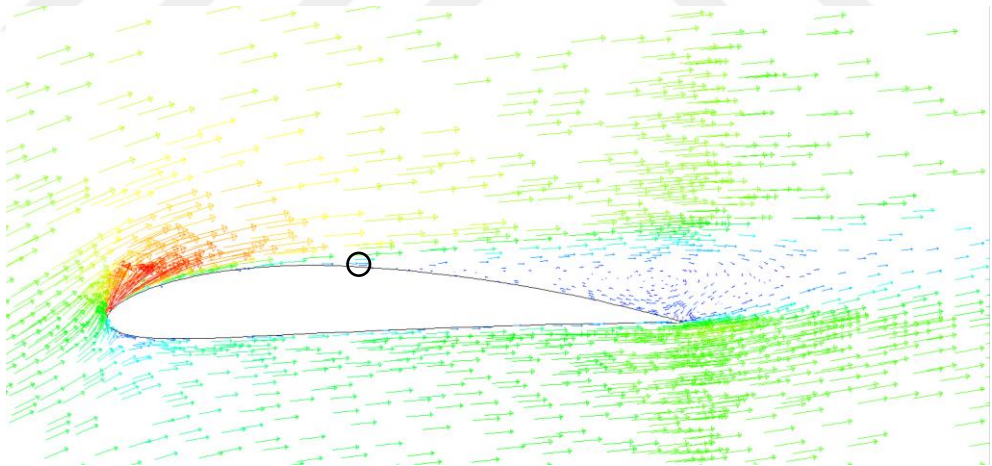


Figure 5.30 Velocity vector of NACA 4412 at 15° AoA

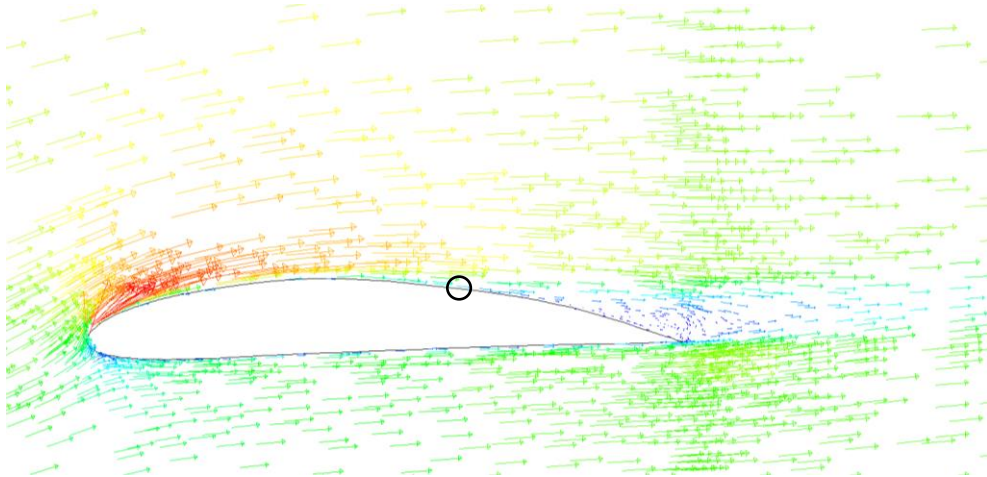


Figure 5.31 Velocity vector of NACA 4412_1 at 15⁰ AoA

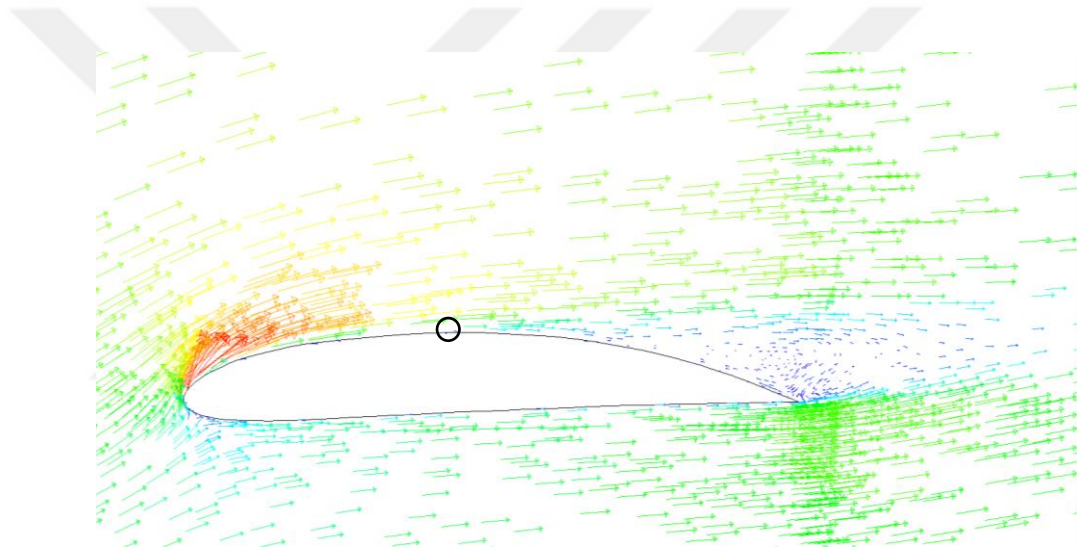


Figure 5.32 Velocity vector of NACA 4412_2 at 15⁰ AoA

When the figure 5.30, 5.31, and 5.32 were investigated it was seen that flow separation started nearly at the middle of the airfoil at 15⁰ AoA.

Velocity vector of NACA 4412, NACA 4412_1, and NACA 4412_2 at 18⁰ AoA value were given in the figure 5.33, 5.34, and 5.35 respectively.

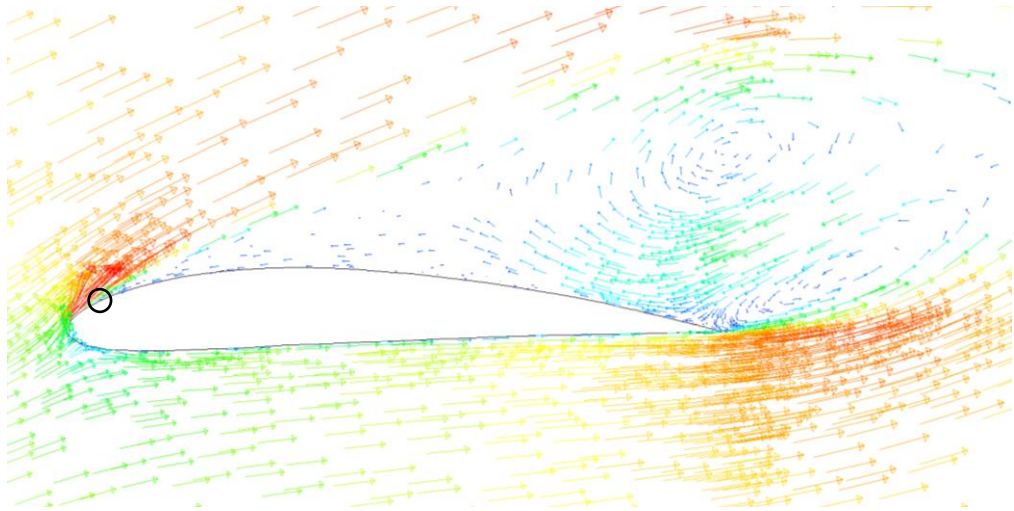


Figure 5.33 Velocity vector of NACA 4412 at 18⁰ AoA

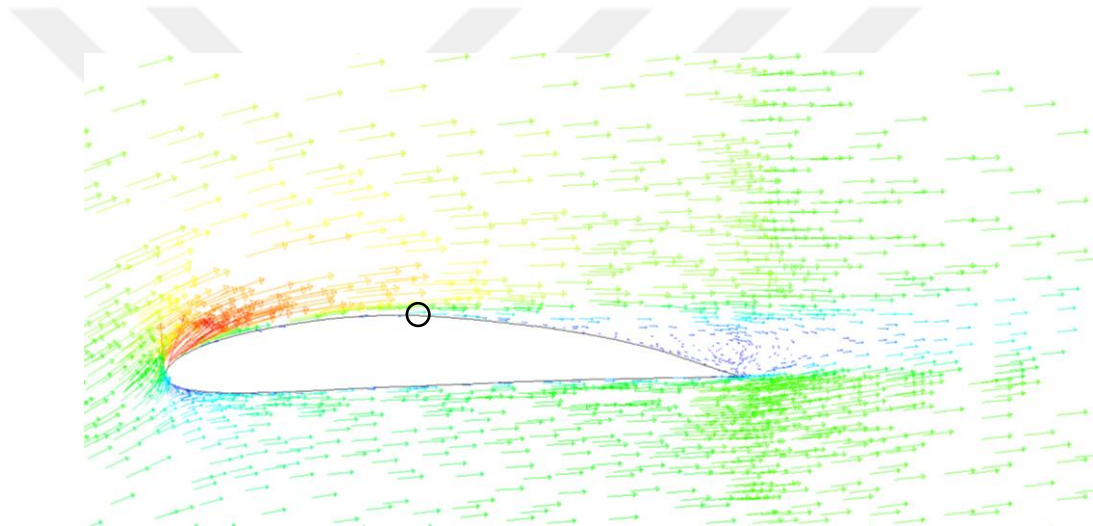


Figure 5.34 Velocity vector of NACA 4412_1 at 18⁰ AoA

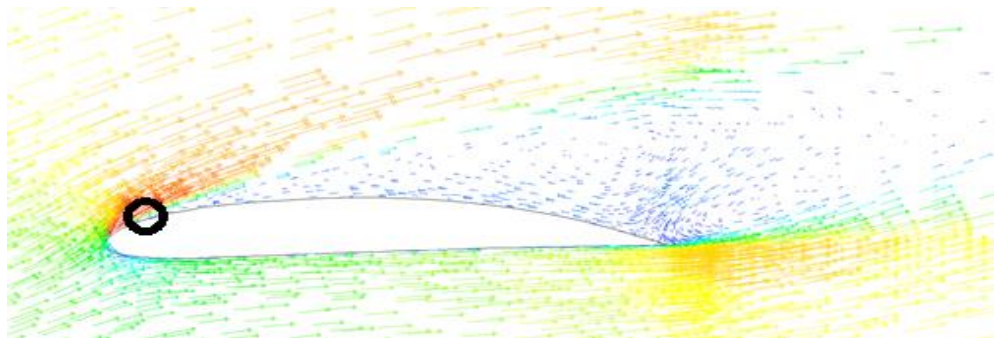


Figure 5.35 Velocity vector of NACA 4412_2 at 18⁰ AoA

When the figure 30, 31, and 32 were investigated it was seen that flow separation started at the front of the airfoil for NACA 4412 and NACA 4412_2 but flow separation started at the middle of the airfoil for NACA 4412_1 at 18⁰ AoA.

Turbulent viscosity of NACA 4412, NACA 4412_1, and NACA 4412_2 at 18° AoA value were given in the figure 5.36, 5.37, and 5.38 respectively.

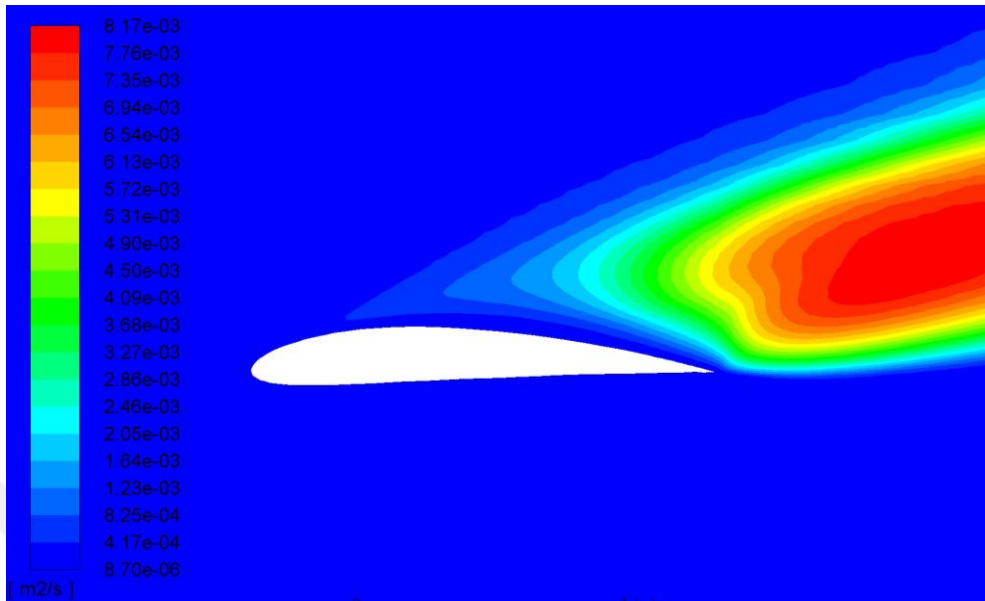


Figure 5.36 Turbulent viscosity of NACA 4412 at 18° AoA

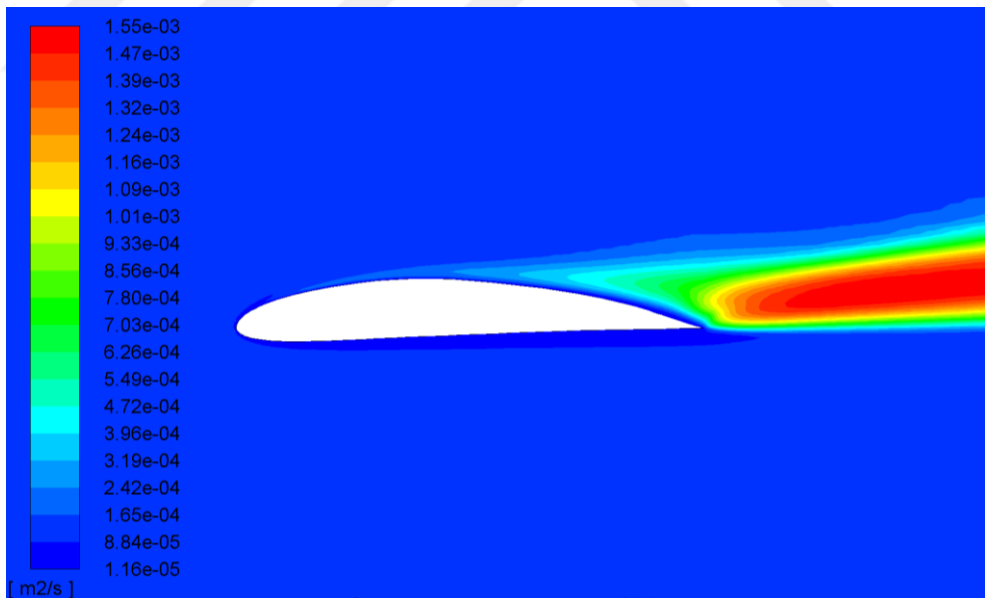


Figure 5.37 Turbulent viscosity of NACA 4412_1 at 18° AoA

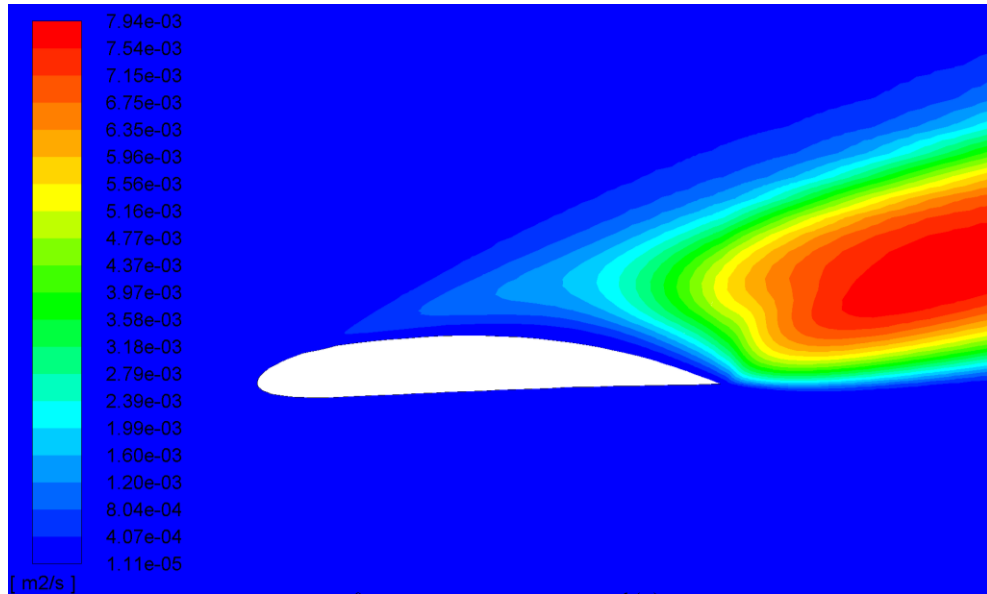


Figure 5.38 Turbulent viscosity of NACA 4412_2 at 18° AoA

After investigation of the analysis results, it was seen that maximum aerodynamic performance was obtained on original NACA 4412 between 0° and 12° AoA, on NACA 4412_2 between 12° and 17° AoA, and on NACA 4412_1 between 17° and 23° AoA. So, it must be used different airfoils during the flight to obtain maximum aerodynamic performance (Göv et. al.).

5.4 Adjustable NACA 63-215 Profile Design

Aerodynamic efficiency of NACA 63-215 airfoil was investigated at various angles of attack (AoA) from 0° to 23°. The coefficient of lift and drag values were calculated for $7,0388 \times 10^4$ Reynolds number.

The computational fluid dynamic (CFD) analysis was used to determine the aerodynamic performance of two-dimensional (2D) flow over airfoils. In this section, aerodynamic performance of the NACA 63-215 and improved NACA 63-215 airfoil (Figure 5.39) was compared. Aerodynamic performance of these 2-airfoils was compared at different AoA (between 0° and 23°) values. Drag coefficient, lift coefficient and flow separation were used as performance parameter.

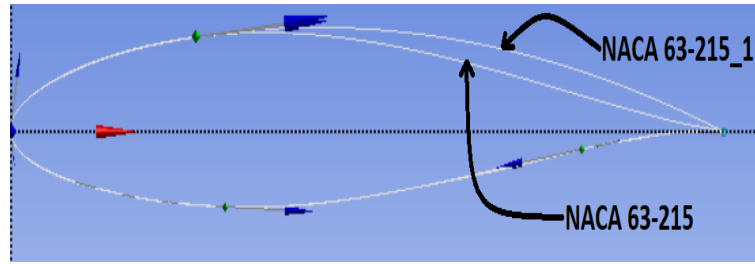


Figure 5.39 NACA 63-215 and improved airfoil NACA 63-215_1

Analysis were performed using CFD tool of ANSYS software, which is commercial finite element analysis program. Complete mesh distribution can be seen in the figure 5.40, enlarged view of NACA 63-215 mesh and enlarged view of improved NACA 63-215 mesh is given in the figure 5. 41.

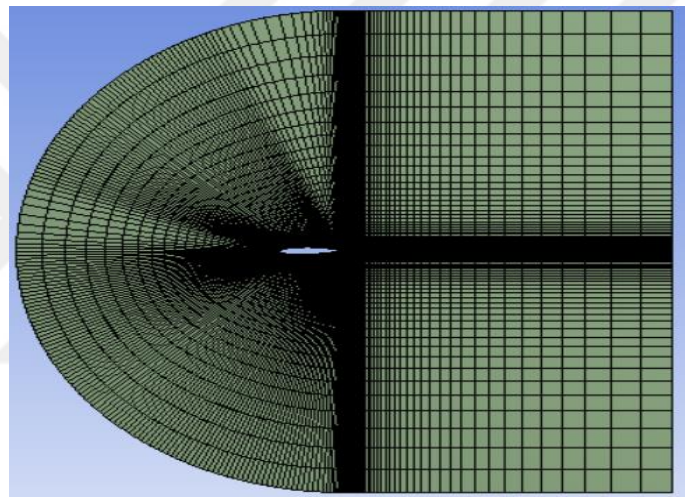
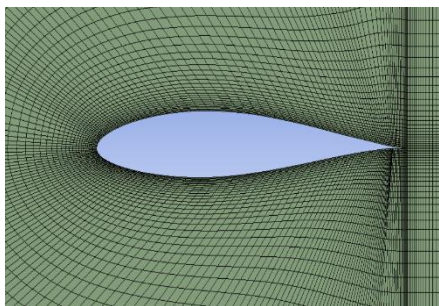
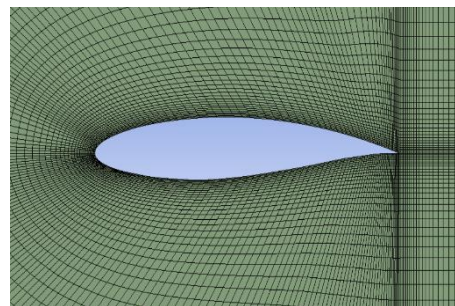


Figure 5.40 Complete mesh



a) NACA 63-215



b) NACA 63-215_1

Figure 5.41 Enlarged view of NACA 63-215 and improved NACA 63-215_1 mesh

Lift coefficients of NACA 63-215 and NACA 63-215_1 at different AoA were given in the figure 5.42. Also, drag coefficients of NACA 63-215 and NACA 63-215_1 at different AoA were given in the figure 5.43.

When figure 5.42 was investigated, it was seen that maximum lift coefficient was obtained at 17° AoA for original NACA 63-215 and minimum lift coefficient was obtained at 0° AoA for original NACA 63-215. Also, maximum lift coefficient was obtained at 21° AoA for NACA 63-215_1 and minimum lift coefficient was obtained at 0° AoA for NACA 63-215_1. So, comparisons of the results were given at these 3 angles of attack values.

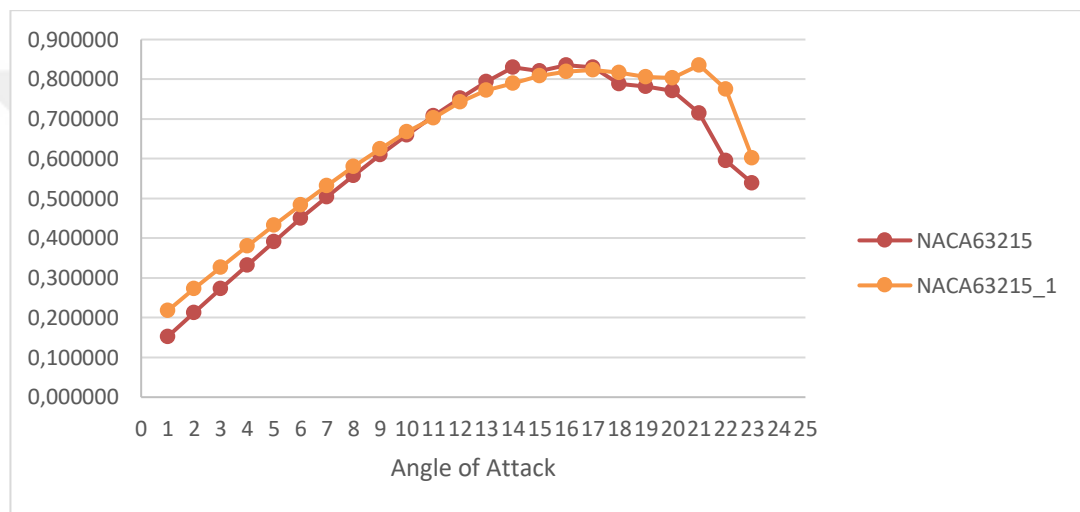


Figure 5.42 Lift coefficient at different AoA

The NACA 63-215 airfoil must be used at 16° and 21° degrees angle of attack, NACA 63-215_1 must be used between 0° - 15° , 17° - 20° and 22° - 23° degrees angle of attack, to obtain maximum lift.

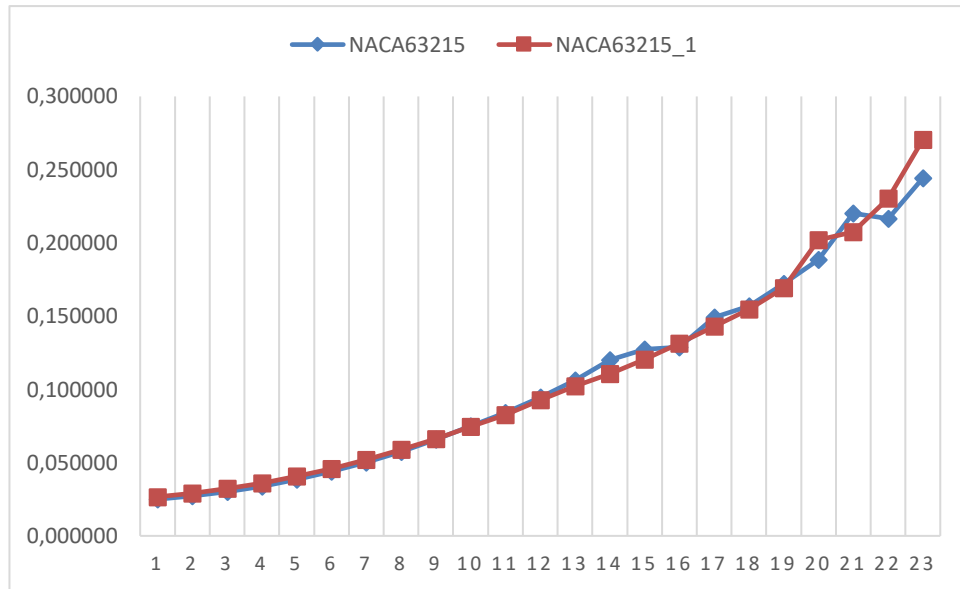


Figure 5.43 Drag coefficient at different AoA

The NACA 63-215 airfoil must be used up to a 12 degree and NACA 63-215_1 must be used up after 12 degree angle of attack, to obtain minimum drag.

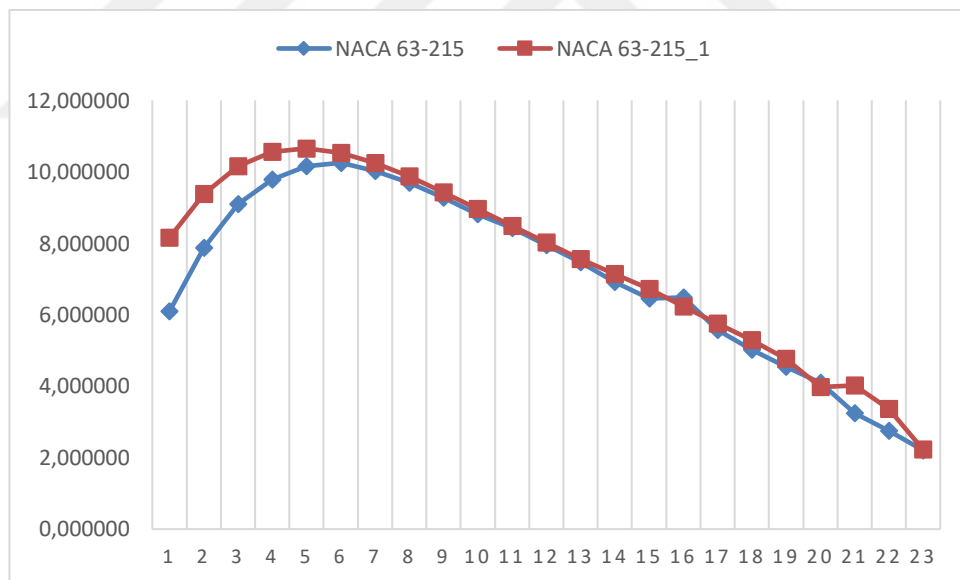


Figure 5.44 Cl/Cd at different AoA

The NACA 63-215 airfoil must be used at 16⁰ and 21⁰ AoA, NACA 63-215_1 must be used between 0⁰-15⁰, 17⁰-20⁰ and 22⁰-23⁰ AoA to obtain maximum aerodynamic efficiency. Cl/Cd ratio was given according to angle of attack in the figure 5.44.

Pressure distribution of NACA 63-215 and NACA 63-215_1 at 0⁰ AoA value were given in the figure 5.45 and 5.46 respectively. Velocity distribution of NACA 63-215

and NACA 63-215_1 at 0° AoA value were given in the figure 5.47 and 5.48 respectively.

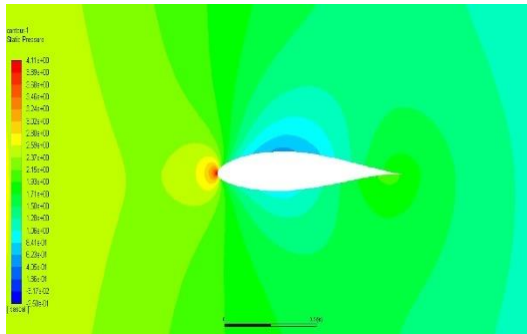


Figure 5.45 Pressure distribution of NACA 63-215 at 0° AoA

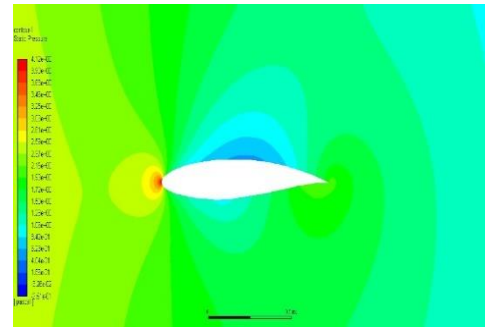


Figure 5.46 Pressure distribution of NACA 63-215_1 at 0° AoA

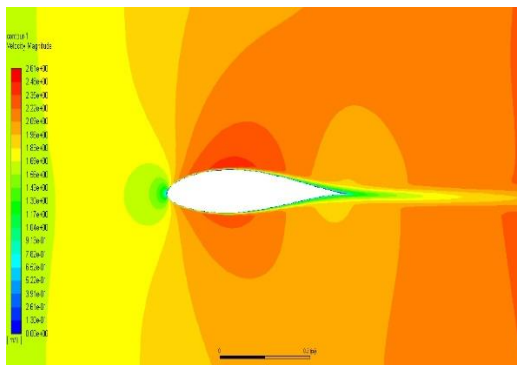


Figure 5.47 Velocity distribution of NACA 63-215 at 0° AoA

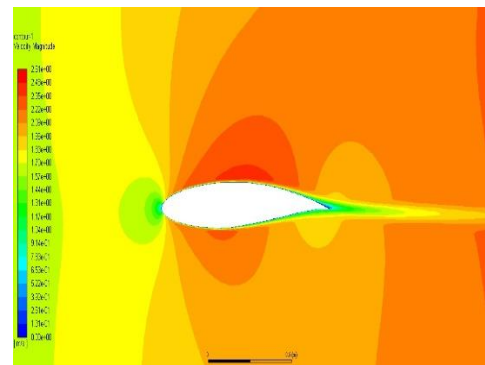


Figure 5.48 Velocity distribution of NACA 63-215_1 at 0° AoA

Pressure distribution of NACA 63-215 and NACA 63-215_1 at 17° AoA value were given in the figure 5.49 and 5.50 respectively. Velocity distribution of NACA 63-215 and NACA 63-215_1 at 17° AoA value were given in the figure 5.51 and 5.52 respectively.

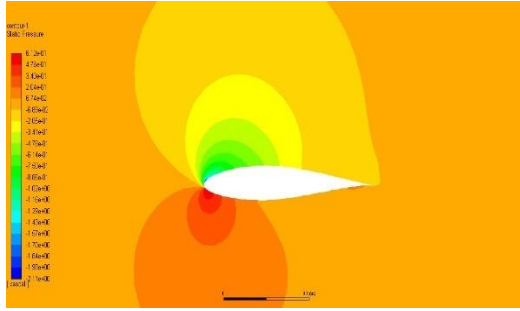


Figure 5.49 Pressure distribution of NACA 63-215 at 17⁰ AoA

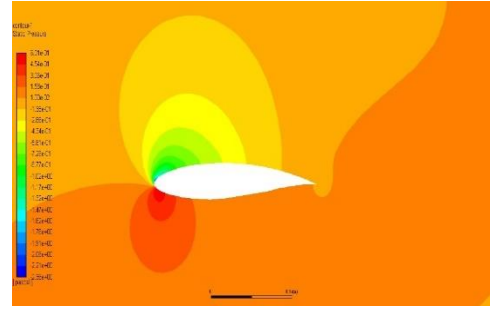


Figure 5.50 Pressure distribution of NACA 63-215_1 at 17⁰ AoA

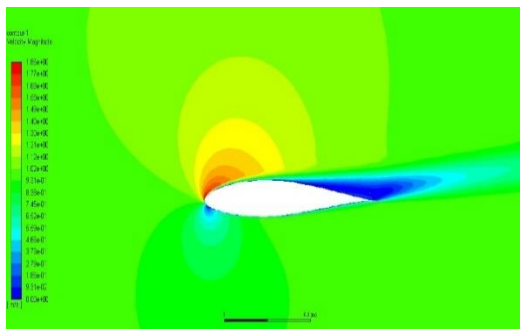


Figure 5.51 Velocity distribution of NACA 63-215 at 17⁰ AoA

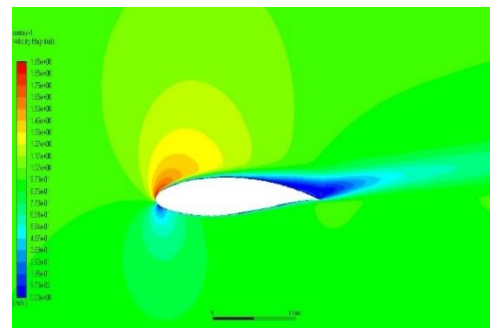


Figure 5.52 Velocity distribution of NACA 63-215_1 at 17⁰ AoA

Pressure distribution of NACA 63-215 and NACA 63-215_1 at 21⁰ AoA value were given in the figure 5.53 and 5.54 respectively. Velocity distribution of NACA 63-215 and NACA 63-215_1 at 21⁰ AoA value were given in the figure 5.55 and 5.56 respectively.

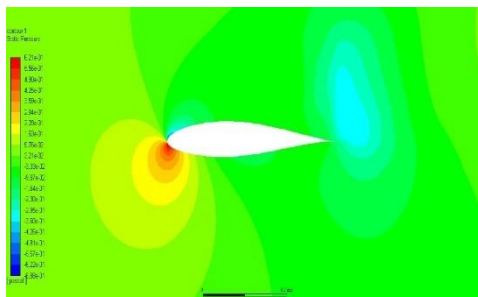


Figure 5.53 Pressure distribution of NACA 63-215 at 21⁰ AoA

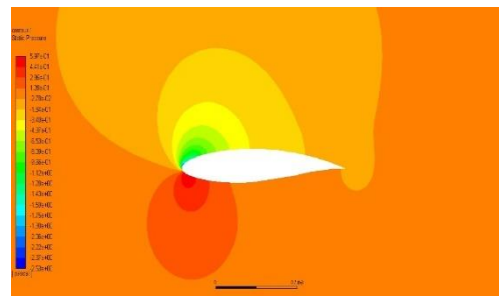


Figure 5.54 Pressure distribution of NACA 63-215_1 at 21⁰ AoA

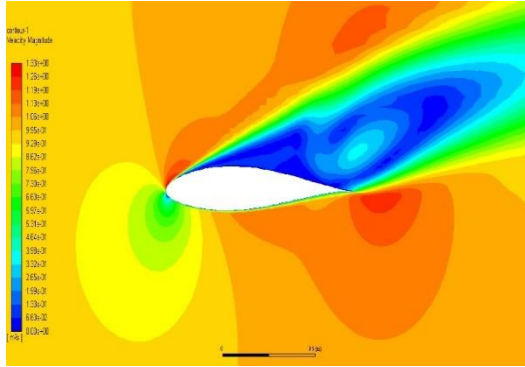


Figure 5.55 Velocity distribution of NACA 63-215 at 21° AoA

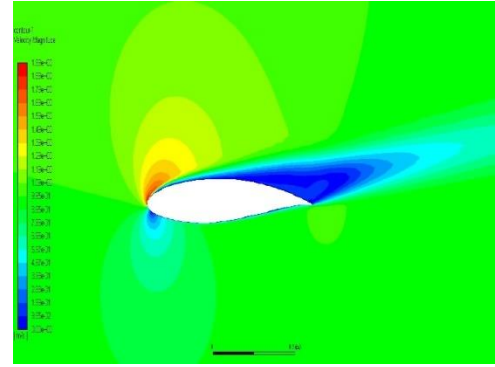


Figure 5.56 Velocity distribution of NACA 63-215_1 at 21° AoA

Velocity vector of NACA 63-215 and NACA 63-215_1 0° AoA value were given in the figure 5.57 and 5.58 respectively.

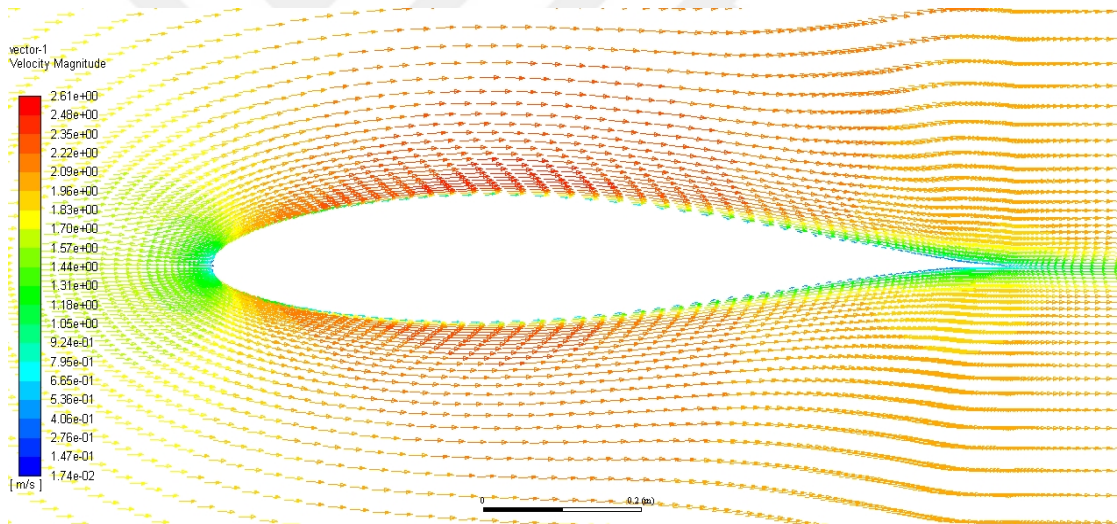


Figure 5.57 Velocity vector of NACA 63-215 at 0° AoA

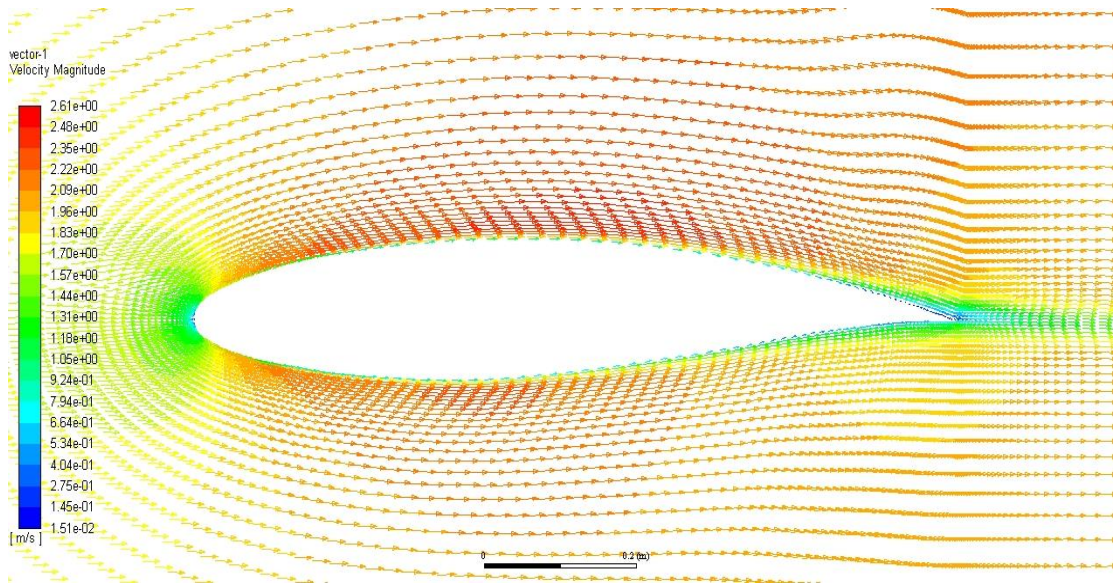


Figure 5.58 Velocity vector of NACA 63-215_1 at 0° AoA

When the figure 5.57 and 5.58 were investigated it was seen that there was no flow separation at 0° AoA.

Velocity vector of NACA 63-215 and NACA 63-215_1 at 17° AoA value were given in the figure 5.59 and 5.60 respectively.

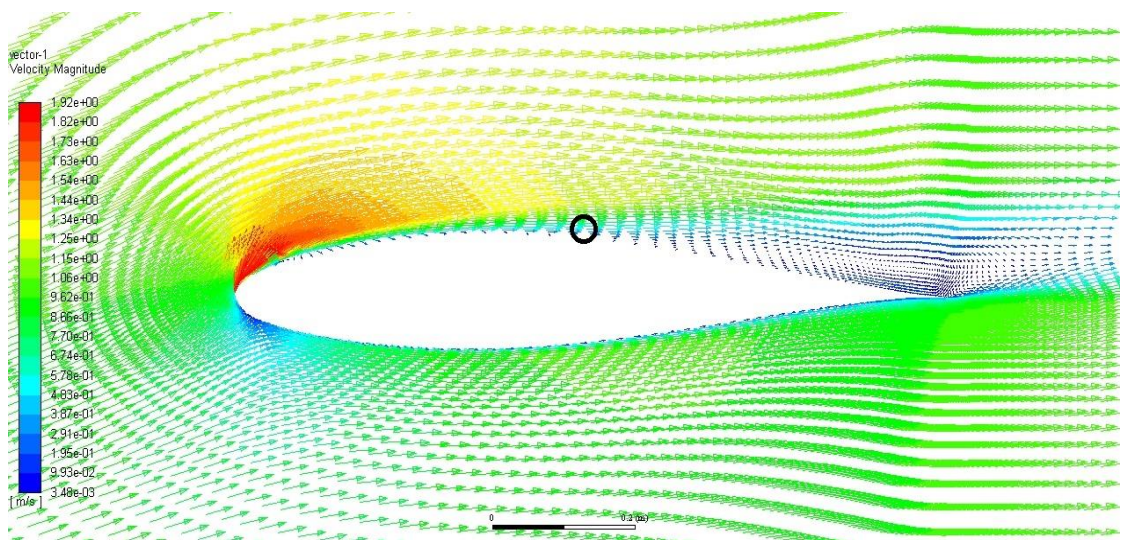


Figure 5.59 Velocity vector of NACA 63-215 at 17° AoA

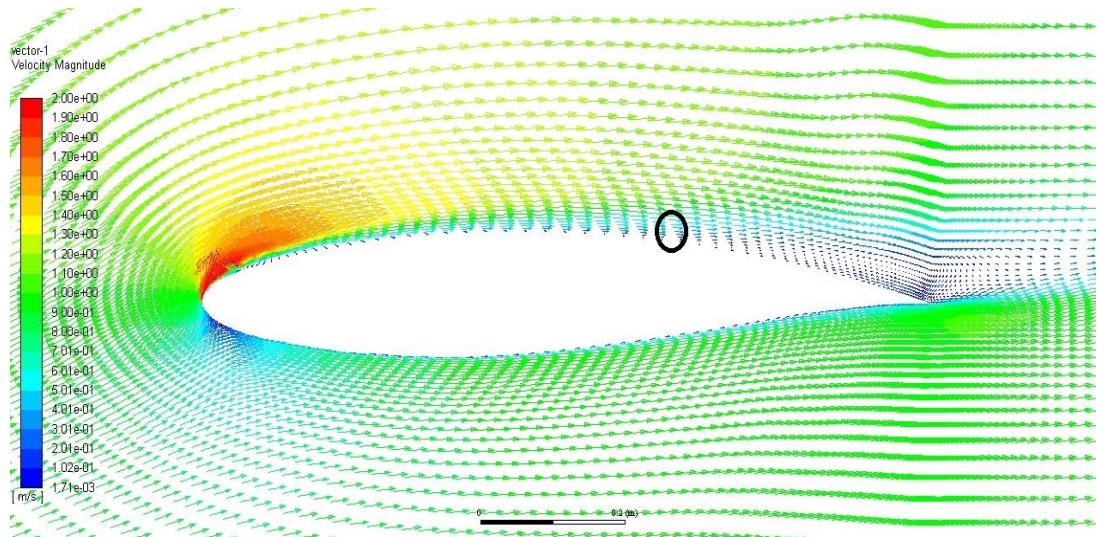


Figure 5.60 Velocity vector of NACA 63-215_1 at 17⁰ AoA

When the figure 59 and 60 were investigated it was seen that flow separation started at the nearly middle of the airfoil for NACA 63-215 but flow separation started at the nearly back of the airfoil for NACA 63-215_1 at 17⁰ AoA.

Velocity vector of NACA 63-215 and NACA 63-215_1 at 21⁰ AoA value were given in the figure 5.61 and 5.62 respectively.

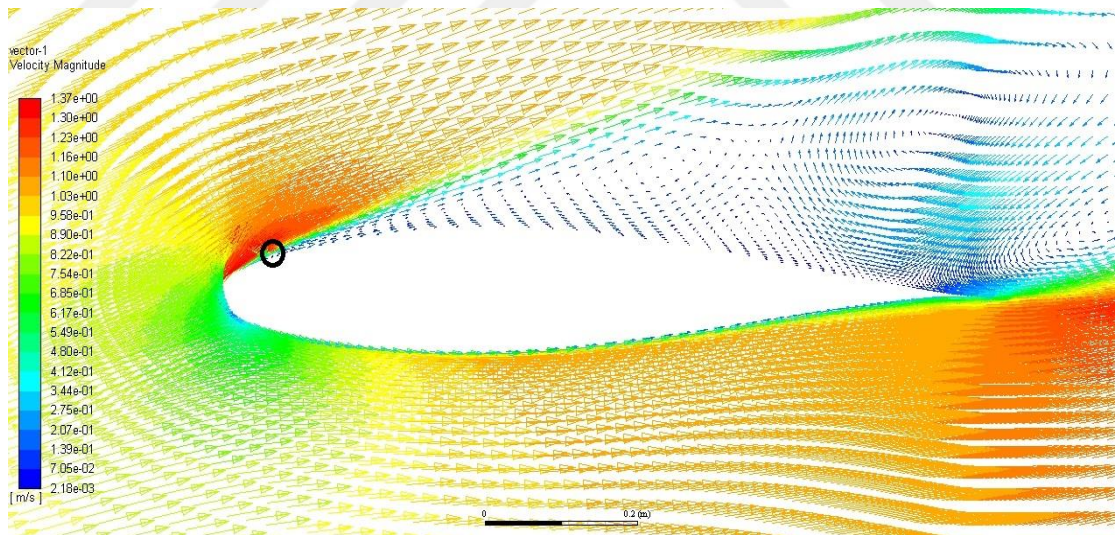


Figure 5.61 Velocity vector of NACA 63-215 at 21⁰ AoA

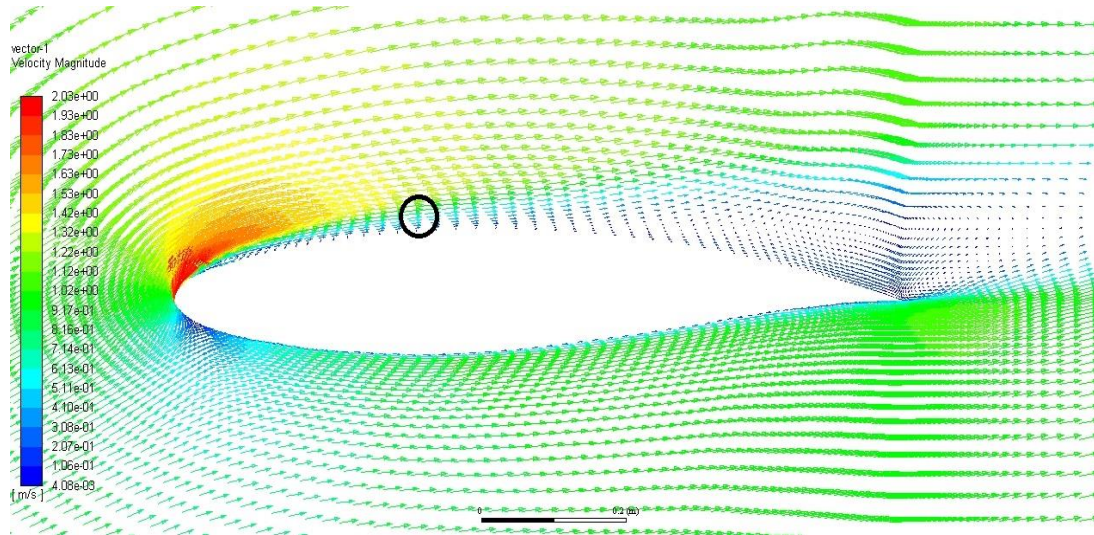


Figure 5.62 Velocity vector of NACA 63-215_1 at 21⁰ AoA

When the figure 61 and 62 were investigated it was seen that flow separation started at the front of the airfoil for NACA 63-215 but flow separation started at the middle of the airfoil for NACA 63-215_1 at 21⁰ AoA.

Turbulent viscosity of NACA 63-215 and NACA 63-215_1 at 17⁰ AoA value were given in the figure 5.63 and 5.64 respectively.

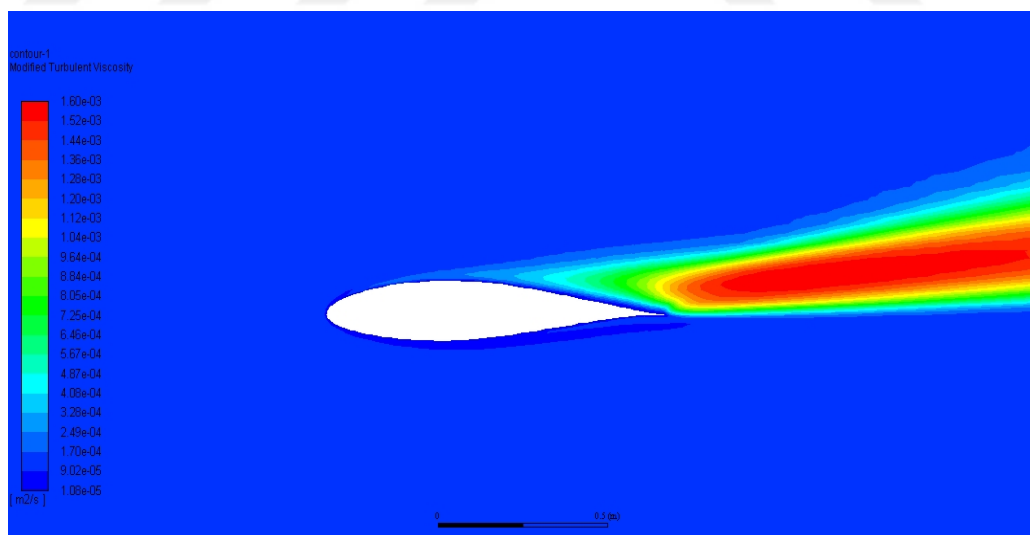


Figure 5.63 Turbulent viscosity of NACA 63-215 at 17⁰ AoA

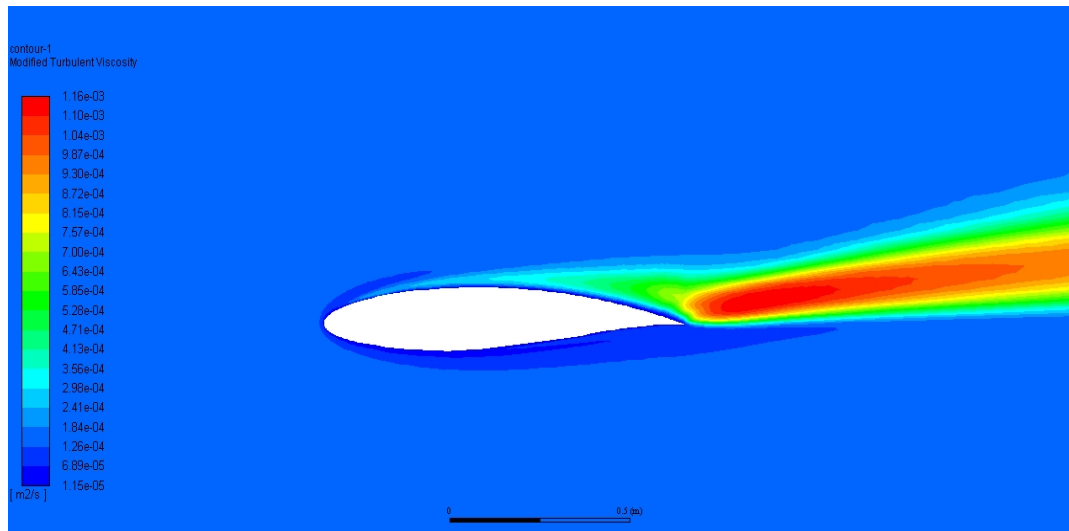


Figure 5.64 Turbulent viscosity of NACA 63-215_1 at 17⁰ AoA

After investigation of the analysis results, it was seen that maximum aerodynamic performance was obtained the NACA 63-215 airfoil must be used at 16⁰ and 21⁰ AoA, NACA 63-215_1 must be used between 0⁰-15⁰, 17⁰-20⁰ and 22⁰-23⁰ AoA to obtain maximum aerodynamic efficiency. Cl/Cd ratio was given according to angle of attack in the figure 5.44. So, it must be used different airfoils during the flight to obtain maximum aerodynamic performance.

CHAPTER 6

RESULTS AND DISCUSSIONS

In this study, improved airfoils were investigated which are NACA 4412 and NACA 63-215. 2 improved airfoils were used to increase the aerodynamic performance of NACA 4412 at different angle of attack values. Aerodynamic performance of these 3-airfoils was compared in terms of the different angle of attack (between 0^0 and 23^0) values. Drag coefficient, lift coefficient and flow separation were used as performance parameter.

After the analysis, the comparison of the results was given below:

- Maximum lift coefficient was obtained:
 - at 15^0 AoA for original NACA 4412
 - at 19^0 AoA for NACA 4412_1
 - at 15^0 AoA for NACA 4412_2
- Minimum lift coefficient was obtained:
 - at 0^0 AoA for original NACA 4412
 - at 0^0 AoA for NACA 4412_1
 - at 0^0 AoA for NACA 4412_2
- Maximum lift coefficient loss was occurred:
 - at 18^0 AoA due to flow separation for original NACA 4412
 - at 20^0 AoA due to flow separation for NACA 4412_1
 - at 18^0 AoA due to flow separation for NACA 4412_2
- There was no flow separation for three airfoils at 0^0 AoA.
- Flow separation started at the middle of the airfoil for three airfoils at 15^0 AoA.
- At 18^0 AoA, flow separation started:
 - at the front of the airfoil for NACA 4412
 - at the middle of the airfoil for NACA 4412_1
 - at the front of the airfoil for NACA 4412_2
- Maximum aerodynamic

- performance was obtained on original NACA 4412 between 0° and 12° AoA, on NACA 4412_2 between 12° and 17° AoA, and on NACA 4412_1 between 17° and 23° AoA.

1 improved airfoils were used to increase the aerodynamic performance of NACA 63-215 at different angle of attack values. Aerodynamic performance of these 2-airfoils was compared in terms of the different angle of attack (between 0° and 23°) values. Drag coefficient, lift coefficient and flow separation were used as performance parameter.

After the analysis, the comparison of the results was given below:

- Maximum lift coefficient was obtained:
 - at 17° AoA for original NACA 63-215
 - at 21° AoA for NACA 63-215_1
- There was no flow separation for three airfoils at 0° AoA.
- Flow separation started at the middle of the airfoil for three airfoils at 12° AoA.
- At 18° AoA, flow separation started:
 - at the middle of the airfoil for NACA 63-215
 - at the back of the airfoil for NACA 63-215_1
- Maximum aerodynamic performance was obtained on original NACA 63-215 at 16° and 21° , on NACA 63-215_1 between 0° - 15° , 17° - 20° and 22° - 23° AoA.
- Finally, the analysis results showed that it must be used different airfoils during the flight to obtain maximum aerodynamic performance.

CHAPTER 7

CONCLUSION

Standard airfoils are designed to provide maximum performance under small range of AoA values. The airfoil performances decrease rapidly outside of this range. Different airfoils are needed to enhance this range in different AoA values during flight. The mechanism designed for the replacement of the wing profile is shown in Fig. 7.1. The control surface is moved through the servomotor and the final position is given to the polymer-based flexible material on the upper side of the wing.

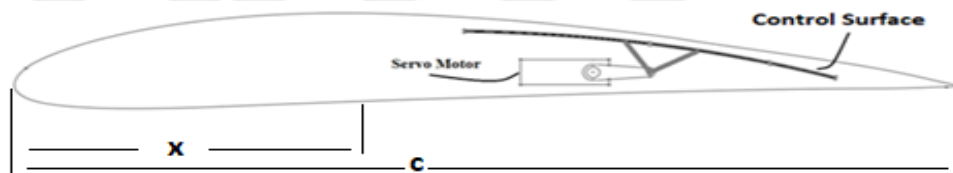


Figure 7.1 Wing profile change mechanism

In this study was used airfoils which have x/c ratio 0.33432 for NACA 63-215 and x/c ratio is 0.41573 for advanced profile NACA 63-215_1. With an increase of 1.12 percent in the maximum lift force, the stall condition was observed to be delayed by 4 degrees for NACA 63-215. When x/c value is ratio 0.34 for normal profile NACA 4412 was increased to 0,52 for NACA 4412_1 and 0,536 for NACA 4412. The maximum lift force obtains at 15° for normal NACA 4412, 19° for NACA NACA4412_1 and 15° for NACA 4412_2. As a result of changing the NACA 4412 airfoil, the increase of the maximum lift force coefficient was determined as 5%.

As a result, the analyzes show that variable airfoils are needed to achieve maximum aerodynamic performance at different attack angles during flight as seen in Fig. 7.2. By using flexible materials on the wing surfaces and the mechanisms that can translate these surfaces into the desired geometry, it will be possible to obtain maximum performance during flight.

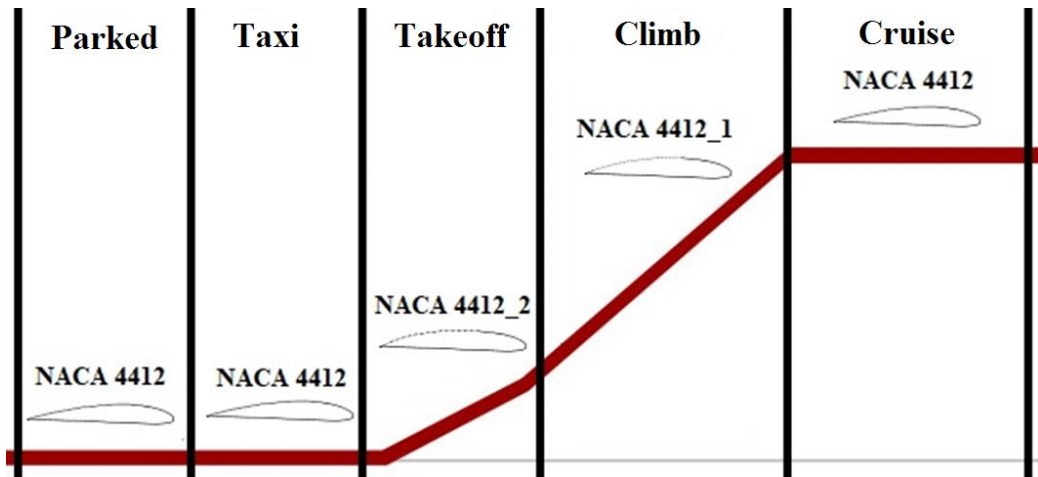


Figure 7.2 Usage of wing profile according to flight



CHAPTER 8

FUTURE WORKS

In this study, effect of the variable airfoils on aerodynamic performance was investigated at different angle of attack values. And the study shows that variable airfoils provided maximum aerodynamic performance.

In the continuation of this study, optimum airfoil will be obtained by aerodynamic optimization.

Also, an experimental study will be performed to show the actual performance of the variable airfoil.

REFERENCES

- Chitte, P., Jadhav, PK., and Bansode, SS. (2013). Statistic and dynamic analysis of typical wing structure of aircraft using Nastran. *International Journal of Application or Innovation in Engineering & Management*. **2**, 49-55.
- Dash, A. (2016). CFD Analysis of Wind Turbine Airfoil at Various Angles of Attack. *IOSR Journal of Mechanical and Civil Engineering*. **13**, 18-24.
- Demir, H., Özden, M., Genç, M. S., Çağdaş, M. (2016). Numerical investigation of flow on NACA4412 airofoil with different aspect ratios. *Physical Journal Conferences*. **114**, 5.
- Findanis, N., Ahmed, N.A. (2008). The interaction of an asymmetrical localised synthetic jet on a side-supported sphere. *Journal of Fluids and Structures*. **24**, 1006-1020.
- Glezer, A., Amitay, M. (2002). Synthetic jets. *Annual Review of Fluid Mechanics*. **34**, 503–529.
- Goodarzi, M., Rahimi, M., Fereidouni R. (2012). Investigation of Active Flow Control over NACA0015 Airfoil Via Blowing. *International Journal of Aerospace Sciences*. **1(4)**, 57-63.
- Gopinathan, V. T., Ganesh, M. (2015). Passive Flow Control over NACA0012 Aerofoil using Vortex Generators. *International Journal of Engineering & Technology IJET*. **4**, Issue 9, September 2015.
- Göv, İ., Doğru, M. H., Korkmaz, Ü. (2018)., Improvement of the aerodynamic performance of NACA 4412 using the adjustable airfoil profile during the flight, *Journal of the Faculty of Engineering and Architecture of Gazi University*. **18(2)** <https://doi.or./10.17341/gazimmfd.460536>.
- Holst, T. L. (1994). Computational Fluid Dynamics Uses in Fluid Dynamics/ Aerodynamics Education. *NASA Technical Memorandum 1994; 108834*. NASA-TM-108834.

- Hossain, MD. S., Raiyan, M. F., Akanda, M. N. U., Jony, N. H. (2014). A Comparative Flow Analysis of NACA 6409 and NACA 4412 Airfoil. *IJRET: International Journal of Research in Engineering and Technology*. **03**, 342-350.
- Jirasek, A. (2005). Vortex-generator model and its application to flow control. *Journal of aircraft*. **42**,1486-1491.
- Justin, P., Ryan, P., Ashok, G., Neal T. F. (2013). A CFD Database for Airfoils and Wings at Post-Stall Angles of Attack. Proc. of the 31st AIAA Applied Aerodynamics Conference. San Diego, CA. No:919.
- Kevadiya, M. (2013). CFD Analysis of Pressure Coefficient for NACA 4412. *International Journal of Engineering Trends and Technology (IJETT)*. **4**, Issue 5, May 2013.
- Kevadiya, M. and Vaidya, HA. (2013). 2D analysis of NACA 4412 airfoil. *International Journal of Innovative Research in Science, Engineering and Technology*. **2**, Issue 5, May 2013.
- Kostića, Č. L. and Rašuo, B. P. (2016) Aerodynamic Airfoil at Critical Angles of Attack. *Military Technical Courier*. **64**, 784-811.
- Kumar, A. (2014). Investigation of Airfoil Design. Unpublished Degree of Bachelor Thesis. National Institute of Technology Rourkela. Odisha, INDIA.
- Lynch, F.T. (1982). Commercial transports-aerodynamic design for cruise performance efficiency in transonic aerodynamics. *Progress in astronautics and aeronautics*, **81**, 81-147.
- Mashud, M. and Ferdous, M. (2012). Flow Separation Control of Thick Airfoil by a Trapped Vortex. *International Journal of Engineering & Technology IJET*. **12**, 1-4.
- Mehmood, N., Liang, Z. and Khan, J. (2012). CFD Study of NACA 0018 for Diffuser Design of Tidal Current Turbines. *Research Journal of Applied Sciences, Engineering and Technology*. **4(21)**, 4552-4560.
- Milano, M., Koumoutsakos, P., Giannakopoulos, X., Schmidhuber, J. (2000). Evolving strategies for active flow control. *Proceedings of the 2000 Congress on Evolutionary Computation*. **1**, 212-218.
- Panda, D. (2015). Computational Fluid Dynamics of Aerofoil Sections. Unpublished Degree of Bachelor Thesis. National Institute of Techonlogy Rourkela. Odisha, INDIA.

- Patel, K. S., Patel, S. B., Patel, U. B., Ahuja, A. P. (2014). CFD Analysis of an Aerofoil. *IJRASET: International Journal of Engineering Research*. **3**, 154-158.
- Sagat, C., Mane, P. and Gawali, B. S. (2012). Experimental and CFD Analysis of Airfoil at Low Reynolds Number. *International Journal of Mechanical Engineering and Robotics Research*. **1**, 277-283.
- Shehata, A. S., Xiao, Q., Saqr, K. M., Naguib, A., Alexander, D. (2017). Passive flow control for aerodynamic performance enhancement of airfoil with its application in Wells turbine – under oscillating flow condition. *Ocean Engineering*. **136**, 31-53.
- Singh, D. K., Jain, A., Paul, A. R. (2016). Active Flow Control on NACA23012 Airfoil using Combined Action of Synthetic Jet and Continuous Jet. Proceedings of the 6th International and 43rd National Conference on Fluid Mechanics and Fluid Power December 15-17, 2016, MNNITA, Allahabad, U.P., India, At Allahabad, India, **43**.
- Tebbiche, H. and Boutoudj, M. S. (2015). Passive Control on the NACA 4412 Airfoil and Effects on the Lift. Design and Modeling of Mechanical Systems-II, Chouchane M., Fakhfakh T., Daly H.B., Aifaoui, N., Chaari, F. (Eds.), 775-781.
- Thibert, J.J., Reneaux, J., Moens, F., Priest, J. (1995). ONERA activities on high lift devices for transport aircraft. *Aeronautical Journal*. **99**, 395–411.
- Tuck, A. and Soria, J. (2004). Active Flow Control over a NACA 0015 Airfoil using a ZNMF Jet. Proceedings of the 15 th Australasian Fluid Mechanics Conference. 13-17 December 2004. The University of Sydney, Sydney, Australia.
- You, D., Moin, P. (2008). Active control of flow separation over an airfoil using synthetic jets. *Journal of Fluids and Structures*. **24**, 1349-1357.